The Annals of Statistics
2023, Vol. 51, No. 5, 2221–2245
https://doi.org/10.1214/23-AOS2332

SPATIAL QUANTILES ON THE HYPERSPHERE

BY DIMITRI KONEN[a] AND DAVY PAINDAVEINE[b]

ECARES and Department of Mathematics, Université libre de Bruxelles, [a]*Dimitri.Konen@ulb.be,* [b]*Davy.Paindaveine@ulb.be*

We propose a concept of quantiles for probability measures on the unit hypersphere $\mathcal{S}^{d-1}$ of $\mathbb{R}^d$. The innermost quantile is the Fréchet median, that is, the L_1-analog of the Fréchet mean. The proposed quantiles $\mu^m_{\alpha,u}$ are directional in nature: they are indexed by a scalar order $\alpha \in [0, 1]$ and a unit vector u in the tangent space $T_m\mathcal{S}^{d-1}$ to $\mathcal{S}^{d-1}$ at m. To ensure computability in any dimension d, our quantiles are essentially obtained by considering the Euclidean (Chaudhuri (*J. Amer. Statist. Assoc.* **91** (1996) 862–872)) spatial quantiles in a suitable stereographic projection of $\mathcal{S}^{d-1}$ onto $T_m\mathcal{S}^{d-1}$. Despite this link with Euclidean spatial quantiles, studying the proposed spherical quantiles requires understanding the nature of the (Chaudhuri (1996)) quantiles in a version of the projective space where all points at infinity are identified. We thoroughly investigate the structural properties of our quantiles and we further study the asymptotic behavior of their sample versions, which requires controlling the impact of estimating m. Our spherical quantile concept also allows for companion concepts of ranks and depth on the hypersphere. We illustrate the relevance of our construction by considering two inferential applications, related to supervised classification and to testing for rotational symmetry.

1. Introduction. For several decades, an intense research activity has been dedicated to the definition of a suitable *multivariate quantile* concept, that is, of a quantile concept for probability measures over $\mathbb{R}^d$, with $d > 1$. It is of course the lack of a canonical ordering in multivariate Euclidean spaces that makes this a challenging problem. We refer, for example, to the review paper Serfling (2002) and to more recent approaches based on quantile regression (Hallin, Paindaveine and Šiman (2010)) or optimal transport (Chernozhukov et al. (2017), Hallin et al. (2021)). Clearly, the problem of defining multivariate quantiles is closely linked to the problems of defining *multivariate depths* (i.e., centrality measures) or *multivariate ranks*. The various proposals in the literature have found key applications in the context of multidimensional growth charts (see, e.g., Wei (2008) or McKeague et al. (2011)), or, more generally, in situations where multiple-output quantile regression methods are relevant.

Despite some recent contributions to the field, one of the most successful multivariate quantile concepts remains the concept of *spatial quantiles* from Chaudhuri (1996), that is defined as follows. For a probability measure P over $\mathbb{R}^d$, the spatial quantile of order α in direction u for P is defined as an arbitrary minimizer of

$$O^P_{\alpha,u}(\mu) := \int_{\mathbb{R}^d} \{\|z-\mu\| - \|z\| - \alpha u'\mu\}\, dP(z). \tag{1.1}$$

Here, $\alpha \in [0, 1)$, u is a unit d-vector and $\|z\| = \sqrt{z'z}$ is the Euclidean norm of $z \in \mathbb{R}^d$. For $\alpha = 0$ (and an arbitrary u), this provides the celebrated *spatial median* (see, e.g., Brown (1983)). The other spatial quantiles are of a directional, center-outward, nature: the larger α, the further away the corresponding (α, u)-quantile, essentially in direction u, from the spatial median. We will use the terminology *spatial quantiles* in the rest of the paper, but

Received June 2022; revised July 2023.
MSC2020 subject classifications. Primary 62R30, 62G99; secondary 62E10, 62G20.
Key words and phrases. Centrality regions, directional statistics, Fréchet medians, multivariate quantiles, spatial quantiles, statistical depth.

these quantiles are sometimes rather referred to as *geometric quantiles*; see, among others, Cheng and De Gooijer (2007), Cardot, Cénac and Zitt (2013), Girard and Stupfler (2015), or Cardot, Cénac and Godichon-Baggioni (2017). Like classical univariate quantiles (to which they reduce in dimension $d = 1$), spatial quantiles characterize the underlying probability measure P; see Theorem 2.5 in Koltchinskii (1997). While several approaches also satisfy this characterization property, spatial quantiles enjoy a number of distinctive advantages: (i) through convex optimization, sample spatial quantiles are easy to compute even in high dimensions; (ii) they allow for detailed asymptotic results, including Bahadur representation and asymptotic normality results (see, e.g., Koltchinskii (1997) and Chaudhuri (1996)), whereas some recent competing approaches offer at best consistency results only; (iii) Similarly, *spatial ranks* and *spatial depth*, namely the concepts of multivariate ranks and depth associated with spatial quantiles, are available in explicit forms, which, unlike for most (if not all) competing concepts, leads to trivial evaluation in the sample case; (iv) Finally, spatial quantiles allow for direct extensions in infinite-dimensional Hilbert spaces, also in the regression framework; see, for example, Chakraborty and Chaudhuri (2014) and Chowdhury and Chaudhuri (2019).

Now, more and more frequently, statistical applications involve data on manifolds. Historically, this has led researchers to extend to manifolds classical Euclidean functionals, the prototypical example being the extension of the Euclidean concept of mean into the concept of *Fréchet mean* (Fréchet (1948)). Nowadays, more involved statistical techniques, such as functional data analysis, are also considered on manifolds, with the primary focus often being on the unit hypersphere $\mathcal{S}^{d-1} = \{x \in \mathbb{R}^d : \|x\| = 1\}$ of $\mathbb{R}^d$; see, for example, Dai and Müller (2018). The present work aims at defining a concept of quantiles on $\mathcal{S}^{d-1}$. As such, it therefore belongs to *directional statistics*;[1] we refer to the monographs Mardia and Jupp (2000) and Ley and Verdebout (2017a). Several concepts of depth have been proposed on the unit sphere (Liu and Singh (1992), Agostinelli and Romanazzi (2013), Pandolfo, Paindaveine and Porzio (2018)), and, quite interestingly, also on general metric spaces (Dai and Lopez-Pintado (2023)). We further refer to Jupp and Kume (2020) for a recent work where transformations related to *distribution functions*, which are of course related to quantile functions, are considered on Riemannian manifolds; see also Wang et al. (2021). Yet the only quantile concept that was explicitly proposed on the hypersphere and investigated as such is the one from Ley, Sabbah and Verdebout (2014), that, however, lacks flexibility and, as we will explain in the sequel, does not characterize the underlying distribution.

The concept of spherical quantiles we propose requires the choice of a reference point that is expected to play the role of the innermost quantile. Since, in Euclidean cases, the innermost quantile is a multivariate median, we take for reference point the Fréchet median, that is, as the L_1-analog of the Fréchet mean. Like Euclidean spatial quantiles, the resulting quantiles $\mu^m_{\alpha,u}$ will be directional in nature: they are indexed by a scalar order α and a unit vector u that here belongs to the tangent space $T_m\mathcal{S}^{d-1}$ to $\mathcal{S}^{d-1}$ at m. Motivated by the nice properties of spatial quantiles in the Euclidean case, we essentially define our quantiles through a stereographic projection of $\mathcal{S}^{d-1}$ from $-m$ (the antipodal point to m) onto $T_m\mathcal{S}^{d-1}$. Since this stereographic projection sends $-m$ "isotropically at infinity" in $T_m\mathcal{S}^{d-1}$, studying the proposed spherical quantiles requires understanding the nature of the Chaudhuri (1996) spatial quantiles in a version of the projective space where all points at infinity are identified. We thoroughly investigate the structural properties of our quantiles and we further study the asymptotic behavior of their sample versions, which requires controlling the impact of estimating m. Our spherical quantile concept also allows for companion concepts of ranks

[1]In order to avoid any confusion, we will rather speak of *spherical statistics* in the sequel and will use the term *"directional"* only to refer to the directional (in u) nature of the various quantiles we consider.

and depth on the hypersphere. We show the relevance of our construction on two inferential applications, related to supervised classification and testing for rotational symmetry.

The outline of the paper is as follows. In Section 2, we first discuss the "univariate" case $\mathcal{S}^1$ and explain what makes the stereographic construction natural to define quantiles on $\mathcal{S}^{d-1}$ for $d > 2$. Then, we carefully define our spherical quantiles and present a result that justifies how this definition treats $-m$, the point that is left aside in the stereographic projection we consider. In Section 3.1: (i) we show that our innermost spatial quantile actually agrees with the Fréchet median chosen as reference point; (ii) we discuss existence and uniqueness of the proposed quantiles, and (iii) we provide a result that characterizes the behavior of extreme quantiles (i.e., the quantiles obtained as $\alpha \to 1$) in each direction u. This allows us to formally define the spherical quantile function in Section 3.2. In Section 4, we introduce a spherical rank function that, under mild conditions, is the inverse map of the quantile function. This rank function, that is intimately related to the gradient condition defining our quantiles, allows us to show in particular that the quantile function characterizes the underlying probability measure. In Section 5, we define a companion concept of depth and discuss its main properties. In Section 6, we focus on the asymptotic properties of the sample version of our quantiles, and establish strong consistency and Bahadur representation results. In Section 7, we show the relevance of the proposed concepts on both aforementioned inferential applications. In Section 8, we provide final comments. All proofs are deferred to the Supplementary Material (Konen and Paindaveine (2023)).

For the sake of convenience, we introduce here some notation that will be used throughout the paper. First, $X =_d Y$ will mean that X and Y are equal in distribution. For $\mu \in \mathcal{S}^{d-1}$, we will denote as $\mathcal{S}^{d-1}_\mu := \mathcal{S}^{d-1} \setminus \{\mu\}$ the unit sphere deprived of μ and as $T_\mu \mathcal{S}^{d-1}$ the $(d-1)$-dimensional vector subspace of $\mathbb{R}^d$ that is parallel to the tangent hyperplane to $\mathcal{S}^{d-1}$ at μ, that is, $T_\mu \mathcal{S}^{d-1} = \{z \in \mathbb{R}^d : \mu' z = 0\}$. We will write $\mathcal{P}_{d-1}$ for the collection of all probability measures on $\mathcal{S}^{d-1}$. We will denote as $\mathbb{I}[A]$ the indicator function of the set or condition A. Throughout, $\mathrm{E}[\cdot]$ will refer to the usual expectation rather than to the Fréchet mean. The d-dimensional identity matrix will be denoted as I_d. By default, all vectors will be column vectors; yet, to keep notation light, we will often omit transpose signs when writing vectors in components—for instance, we will write $(\cos t, \sin t)$ and $(0, 0, 1)$ instead of $(\cos t, \sin t)'$ and $(0, 0, 1)'$, respectively.

2. Spherical spatial quantiles. In this section, we will define our concept of quantiles on the unit hypersphere $\mathcal{S}^{d-1}$ and justify the choices made in this definition. For these purposes, we start by discussing the circular case $d = 2$, that is, the case of the unit circle $\mathcal{S}^1 = \{(\cos t, \sin t) : t \in [0, 2\pi)\}$, and then turn to the general case $d \geq 2$.

2.1. *Circular quantiles.* Fix $P \in \mathcal{P}_1$ and let the random variable T, with values in $[0, 2\pi)$, be such that $X := (\cos T, \sin T)$ has distribution P. Since the circle is a one-dimensional object, quantiles on the circle can in principle be defined from quantiles on the real line, that is, quantiles of X can in principle be defined from quantiles of T. Yet, interestingly, the circle already presents several key issues we will need to address in higher dimensions. An important issue is the lack of a canonical reference point $m = (\cos t_m, \sin t_m)$ on the circle. For any such reference point, one could, for example, accumulate probability mass above t_m, leading to the circular quantiles $\mu^m_\tau = (\cos q^m_\tau, \sin q^m_\tau)$, $\tau \in [0, 1]$, with q^m_τ the usual τ-quantile of T_m, where T_m is the random variable with values in $[t_m, t_m + 2\pi)$ such that $X =_d (\cos T_m, \sin T_m)$. This, however, cannot be generalized to higher dimensions where it is unclear what it means to accumulate probability mass "above" some reference point on $\mathcal{S}^{d-1}$ with $d > 2$. With this future extension to higher dimensions in mind, it is therefore better to choose a reference point m that will play the role of the innermost quantile, namely the median. In this spirit, a natural candidate for a reference point of this type is a *Fréchet median* $m = (\cos t_m, \sin t_m)$, that minimizes the expected arc length between X and m; see Definition 2.1 below. Parallel as above, one may then define the resulting circular quantiles as $\mu_\tau^m = (\cos q_\tau^m, \sin q_\tau^m)$, $\tau \in [0, 1]$, now with q_τ^m the τ-quantile of the random variable $\tilde{T}_m$, with values in $[t_m - \pi, t_m + \pi)$, such that $X =_d (\cos \tilde{T}_m, \sin \tilde{T}_m)$. Provided that $P[\{-m\}] = 0$, the resulting *circular median* $\mu_{1/2}^m$ then very naturally coincides with the Fréchet median m that was used as reference point.

These circular quantiles using a Fréchet median as a reference point are clearly satisfactory when (a) P admits a unique Fréchet median m and when (b) $P[\{-m\}] = 0$, that is, when $\tilde{T}_m$ does not charge $t_m - \pi$. The issue (a) is a structural one on the circle: for distributions on the real line, the medians (i.e., the minimizers of expected absolute deviations) always form a bounded interval, so that a unique median can always be identified (e.g., as the center of this interval). In contrast, the topology of the circle allows for distributions with sets of Fréchet medians that are disconnected (for instance, when $X = (\cos T, \sin T)$, where T is uniform over $\bigcup_{k=1}^3 [(2k - 1)\pi/3 - \pi/6, (2k - 1)\pi/3 + \pi/6]$, the set of Fréchet medians is $\bigcup_{k=1}^3 \{(2k - 1)\pi/3\}$). In the sequel, we exclude (at least in the population case) these exceptional distributions for which the Fréchet median is nonunique. To address issue (b), it is natural to define $\mu_\tau^m = (\cos q_\tau^m, \sin q_\tau^m)$, where q_τ^m is the τ-quantile of $\tilde{T}_m$, and $\tilde{T}_m$ is still such that $X =_d (\cos \tilde{T}_m, \sin \tilde{T}_m)$ but now takes values in $[t_m - \pi, t_m + \pi]$ and satisfies $P[\tilde{T}_m = t_m - \pi] = P[\tilde{T}_m = t_m + \pi] = P[\{-m\}]/2$. Not only does this choice respect the symmetry of the circle with respect to m, but it also guarantees that the resulting circular median $\mu_{1/2}^m$ coincides with the Fréchet median m even when $P[\{-m\}] > 0$. The issue of such an atom at $-m$ will also need to be carefully dealt with in higher dimensions.

2.2. *Hyperspherical quantiles.* Parallel to the multivariate Euclidean case described in the Introduction, our hyperspherical quantiles will be points of $\mathcal{S}^{d-1}$ indexed by a scalar magnitude α and a direction u. In the sequel, this direction u will be relative to *a reference point m*, that is expected to play the role of the median (the innermost quantile). This is in line with the Euclidean case, where spatial quantiles are thought to be in direction *u from the spatial median* (although such localization is actually superfluous in $\mathbb{R}^d$ as, for fixed u, the half-lines $\{\mu + ru : r \geq 0\}$ "reach" the same point at infinity irrespective of their origin μ). As a reference point on the sphere, we will use a *Fréchet median*.

DEFINITION 2.1. A *Fréchet median* of $P (\in \mathcal{P}_{d-1})$ is any point $m \in \mathcal{S}^{d-1}$ that minimizes the objective function

$$\mu \mapsto g_P(\mu) := \int_{\mathcal{S}^{d-1}} d(\mu, x)\, dP(x) \tag{2.1}$$

over $\mathcal{S}^{d-1}$, where $d(x, y) = \arccos(x'y)$ is the geodesic distance between x and y.

Lebesgue's dominated convergence theorem ensures that g_P is continuous over $\mathcal{S}^{d-1}$, so that, from compactness of $\mathcal{S}^{d-1}$, any $P \in \mathcal{P}_{d-1}$ admits at least one Fréchet median. As already mentioned when discussing the case $d = 2$, uniqueness is not guaranteed in general, and we will assume (tacitly) that uniqueness holds. This assumption is standard in the population case and it is met almost surely in the sample case when observations are sampled from a probability measure that admits a density with respect to the surface area measure on $\mathcal{S}^{d-1}$; see Theorem 4.15 from Yang (2011).[2] On another note, we will show later that we

[2]In Definition 2.2, it is thus only to cover the exceptional cases where the Fréchet median would not be unique in the sample case where we introduce a concept of spherical spatial quantiles that is explicitly relative to a given Fréchet median m. While most results of the paper are stated under the assumption that the Fréchet median is unique, we stress that, under nonuniqueness, they remain valid for an arbitrary Fréchet median.

must have $P[\{m\}] \geq P[\{-m\}]$. (This actually follows from the gradient condition associated with the minimization problem defining m; see Lemma S.3.1.[3])

The discussion at the beginning of this section suggests that spherical quantiles should be defined in direction u from m, which motivates taking u as a unit vector in the "tangent" vector space $T_m\mathcal{S}^{d-1}$ to $\mathcal{S}^{d-1}$ at m. Consider then the stereographic projection of $\mathcal{S}^{d-1}$ from $-m$ onto $T_m\mathcal{S}^{d-1}$, namely the diffeomorphic transformation

$$\pi_m : \mathcal{S}^{d-1}_{-m} \to T_m\mathcal{S}^{d-1} : x \mapsto \pi_m(x) := \frac{x - (m'x)m}{1 + m'x}, \tag{2.2}$$

and let P_{-m} be the probability measure induced by P on $\mathcal{S}^{d-1}_{-m}$, that is, the probability measure defined by $P_{-m}[B] = P[B]/P[\mathcal{S}^{d-1}_{-m}]$ for any Borel set B of $\mathcal{S}^{d-1}_{-m}$ (note that $P[\mathcal{S}^{d-1}_{-m}] = 0$ is excluded, as it would imply that $-m$ is the only Fréchet median of P). In a nutshell, our spherical quantiles are defined by first considering the (Euclidean) spatial quantiles in $\mathbb{R}^d$ of the push-forward image $\pi_m\#P_{-m}$ of P_{-m} by the projection π_m, and then by pulling the resulting quantiles back onto $\mathcal{S}^{d-1}_{-m}$ through π_m^{-1}. More precisely, we adopt the following definition, that also takes into account a possible atom at $-m$.

DEFINITION 2.2. Fix $P \in \mathcal{P}_{d-1}$, with $d \geq 2$, and let m be a Fréchet median of P. Fix $\alpha \in [0, 1]$ and a unit vector u in $T_m\mathcal{S}^{d-1}$. (i) For $\alpha \in [0, p_m)$, with $p_m := 1 - P[\{-m\}]$, we say that $\mu^m_{\alpha,u} = \mu^m_{\alpha,u}(P)$ is an *m-spatial quantile of order α in direction u for P* if and only if it minimizes the objective function

$$\begin{aligned}\mu \mapsto M^{m,P}_{\alpha,u}(\mu) &:= O^{\pi_m\#P_{-m}}_{\alpha/p_m,u}(\pi_m(\mu)) \\ &= \int_{\mathcal{S}^{d-1}_{-m}} \{\|\pi_m(x) - \pi_m(\mu)\| - \|\pi_m(x)\| - \alpha u'\pi_m(\mu)/p_m\} dP_{-m}(x)\end{aligned}$$

over $\mathcal{S}^{d-1}_{-m}$; the m-spatial quantiles of P associated to an order $\alpha = 0$ are called *m-spatial medians* of P. (ii) For $\alpha \in [p_m, 1]$, we let $\mu^m_{\alpha,u} = \mu^m_{\alpha,u}(P) = -m$.

Some comments are in order. Assume first that P does not charge $-m$, so that $p_m = 1$. Then Definition 2.2 implies that $\mu^m_{\alpha,u} (\in \mathcal{S}^{d-1}_{-m})$ is an m-spatial quantile of order $\alpha (< 1)$ in direction u for P if and only if $\pi_m(\mu^m_{\alpha,u})$ is a spatial quantile of order α in direction u for the push-forward probability measure $\pi_m\#P$ in $\mathbb{R}^d$ (formally, this will be a corollary of Lemma S.1.1). Since π_m is a one-to-one map from $\mathcal{S}^{d-1}_{-m}$ to $T_m\mathcal{S}^{d-1}$, the spherical quantile $\mu^m_{\alpha,u}$ is then the inverse image by π_m of the corresponding quantile for $\pi_m\#P$. While this makes Definition 2.2 natural when P does not charge $-m$, it may seem more opaque when $-m$ is an atom of P. This motivates the following result that will explain why our concept is as natural in the latter case as in the former one. To state the result, we recall that a probability measure P over $\mathcal{S}^{d-1}$ is said to be rotationally symmetric about $\mu (\in \mathcal{S}^{d-1})$ if and only if $O\#P = P$ for any $d \times d$ orthogonal matrix such that $O\mu = \mu$.

THEOREM 2.1. *Fix $P \in \mathcal{P}_{d-1}$, with $d \geq 3$, and let m be the Fréchet median of P with $P[\{-m\}] > 0$. Fix $\alpha \in [0, 1]$ and a unit vector u in $T_m\mathcal{S}^{d-1}$. Assume that P is not concentrated on a great circle containing m (which ensures existence and uniqueness of $\mu^m_{\alpha,u}(P)$; see Theorem 3.1 below). Let (Q_ℓ) be a sequence in $\mathcal{P}_{d-1}$ such that*:

(i) *Q_ℓ is rotationally symmetric about m,*
(ii) *there exists $c > 0$ such that $Q_\ell[\{x : d(m, x) < c\}] = 0$ for any ℓ,*

[3]Cross-references of the form Lemma S.m.n or equation (S.m.n) refer to the Supplementary Material.

(iii) $Q_\ell(\{-m\}) = 0$, *and*

(iv) Q_ℓ *converges weakly to the Dirac probability measure at* $-m$.

Then, letting $P_\ell := p_m P_{-m} + (1 - p_m)Q_\ell$, *still with* $p_m = 1 - P[\{-m\}](< 1)$,

$$\mu^m_{\alpha,u}(P_\ell) \to \mu^m_{\alpha,u}(P) \tag{2.3}$$

as ℓ *diverges to infinity.*

As already mentioned, Definition 2.2 above is most natural for probability measures that do not charge $-m$, so that the quantiles $\mu^m_{\alpha,u}(P_\ell)$ in this result are the natural ones. Since the sequence of probability measures (P_ℓ) is defined in such a way that it converges weakly to P (which on the contrary charges $-m$), the "continuity" result in (2.3) actually justifies Definition 2.2 when $P[\{-m\}] > 0$ (equivalently, when $p_m < 1$). Note that this legitimates this definition for both $\alpha \in [0, p_m)$ and $\alpha \in [p_m, 1]$, as all values of α are covered by Theorem 2.1.

No stereographic projection was used in the definition of the circular quantiles in Section 2.1. Yet it is easy to check that the quantiles $\mu^m_{\alpha,u}$ from Definition 2.2 reduce, for $d = 2$, to the circular quantiles defined at the end of Section 2.1, provided of course that the latter are reparametrized according to the center-outward indexing adopted in the present subsection. To be more precise, denote as $m = (\cos t_m, \sin t_m)$ the Fréchet median on the unit circle and consider the random variable $\tilde{T}_m$ with values in $[t_m - \pi, t_m + \pi]$ such that $(\cos \tilde{T}_m, \sin \tilde{T}_m)$ has distribution P and such that $P[\tilde{T}_m = t_m - \pi] = P[\tilde{T}_m = t_m + \pi] = P[\{-m\}]/2$. Then, for any $\alpha \in [0, 1]$ and unit vector u in $T_m\mathcal{S}^1$, the quantile $\mu^m_{\alpha,u}$ from Definition 2.2 coincides with $(\cos q^m_\tau, \sin q^m_\tau)$, where q^m_τ is the $\tau = (\alpha s_u + 1)/2$-quantile of $\tilde{T}_m$; here, $s_u = 1$ (resp., $s_u = -1$) if u indicates the counterclockwise (resp., clockwise) direction on $\mathcal{S}^1$. In particular, for both quantiles in Definition 2.2 and circular quantiles defined at the end of Section 2.1, the quantiles associated with $\alpha \in [p_m, 1]$ in both directions u and $-u$—equivalently, the quantiles associated with $\tau \in [0, (1 - p_m)/2] \cup [(1 + p_m)/2, 1]$—are equal to $-m$. As a consequence, when there is an atom in $-m$, Definition 2.2 is natural in dimension $d = 2$, too (note that this case was not covered by Theorem 2.1). Since the case $d = 2$ only involves univariate Euclidean quantiles, and hence is well understood, we will restrict to the case $d \geq 3$ when studying the proposed spherical quantiles in the next section.

Before proceeding, we close this section with the following important point: while our construction could, in principle, have used any Euclidean multivariate quantile concept in the tangent space $T_m\mathcal{S}^{d-1}$ above, spatial quantiles show a number of distinctive properties that make them the most promising option. First, Euclidean spatial quantiles are objects that involve both a magnitude (α) and a directional component (u), hence provide richer information than quantile/depth functionals that only involve a magnitude component, such as, for example, the Tukey (1975) half-space depth or Liu (1990) simplicial depth. Second, as a corollary of this richer information, spatial quantiles do characterize the underlying distribution, as one would expect for a suitable quantile concept (note that while this has for long been an open question, the half-space depth does not meet this characterization property; see Nagy (2021)). Third, spatial quantiles, and its companion concepts of ranks and depth, can be computed very efficiently in virtually any dimension d. As we will see in the sequel, these nice properties transfer to the proposed spherical spatial quantiles. Even better, since affine transformations make little sense on spheres, our spherical spatial quantiles will actually not suffer from what is considered as the main drawback of (Euclidean) spatial quantiles, namely their lack of affine equivariance.

3. Basic properties of spherical quantiles and the spherical quantile function. We now provide some basic properties for the spherical quantiles introduced in the previous section, which will allow us to define and study the corresponding *spherical quantile function*.

3.1. *Basic properties of spherical quantiles.* We first answer the important questions of existence and uniqueness. We have the following result.

THEOREM 3.1. *Fix $P \in \mathcal{P}_{d-1}$, with $d \geq 3$, and let m be the Fréchet median of P. Fix $\alpha \in [0, 1]$ and a unit vector u in $T_m\mathcal{S}^{d-1}$. Then* (*i*) *P admits an m-spatial quantile $\mu^m_{\alpha,u}$ of order α in direction u*; (*ii*) *if P is not concentrated on a great circle containing m, then $\mu^m_{\alpha,u}$ is unique*; (*iii*) *if P is concentrated on a great circle $\mathcal{C}$ containing m, then uniqueness of $\mu^m_{\alpha,u}$ may fail only if u belongs to the two-dimensional plane containing $\mathcal{C}$ and is tangent to $\mathcal{C}$ at m.*

This result shows that existence always holds and that uniqueness may only fail when P is concentrated on a great circle containing m. But if P is concentrated on a great circle of $\mathcal{S}^{d-1}$ with $d \geq 3$, then P, after a suitable rotation, is actually a probability measure over the unit circle $\mathcal{S}^1 \times \{0\} \subset \mathbb{R}^2 \times \mathbb{R}^{d-2}$, which only requires circular quantiles. Thus, as soon as the problem genuinely requires (hyper)spherical quantiles (because P is not concentrated on a unit circle), we are allowed to speak of *the* m-quantile $\mu^m_{\alpha,u}(P)$ for any $\alpha \in [0, 1]$ and any unit vector u in $T_m\mathcal{S}^{d-1}$.

As explained in the previous section, our spherical quantile concept uses the Fréchet median m as reference point, that is *expected* to be the innermost quantile. From Definition 2.2, however, it is unclear that the resulting innermost quantile, namely the m-spatial median, coincides with the Fréchet median m. The following result shows that this is indeed the case.

THEOREM 3.2. *Fix $P \in \mathcal{P}_{d-1}$ and denote as m the Fréchet median of P. Then m is an m-spatial median of P.*

This result is very general in the sense that it also covers the case where there may be several m-spatial medians, which as explained below Theorem 3.1, is exceptional. In situations where all quantiles are unique, this result naturally states that the Fréchet median m that is used as reference point is the unique m-median, which confirms that this reference point is then *the* innermost quantile for the proposed concept.

We now turn our attention to the high-order quantiles obtained as $\alpha \to p_m$ from below (it is superfluous to consider quantiles with even higher orders since, for any $\alpha \geq p_m$, one has $\mu^m_{\alpha,u} = -m$ irrespective of u). In the Euclidean case, where there cannot be mass at infinity (so that high-order quantiles are obtained as $\alpha \to 1$): (i) high-order spatial quantiles exit any compact subset of $\mathbb{R}^d$ and (ii) they eventually do so in direction u, in the sense that the inner product between u and the unit vector proportional to these quantiles converges to one; see Theorem 2.1 in Girard and Stupfler (2017) for nonatomic measures and Theorems 2–3 in Paindaveine and Virta (2021) for general ones. In the spherical case, we have the following result.

THEOREM 3.3. *Fix $P \in \mathcal{P}_{d-1}$, with $d \geq 3$, and let m be the Fréchet median of P. Assume that P is not concentrated on a great circle containing m. Let (α_n) be a sequence in $[0, p_m)$ that converges to p_m and (u_n) a sequence of unit vectors in $T_m\mathcal{S}^{d-1}$. Then* (*i*) *$\mu^m_{\alpha_n,u_n} \to -m$ and* (*ii*) *if $(u_n) \to u$ for some u, then the unit vector v_n providing the direction in which $\mu^m_{\alpha_n,u_n}$ is to be found from m (defined as the unit vector v_n in $T_m\mathcal{S}^{d-1}$ such that $\mu^m_{\alpha_n,u_n}$ belongs to the great half-circle $\{(\cos t)m + (\sin t)v_n : t \in [0, \pi]\}$) converges to u.*

In the Euclidean case, there is no guarantee that the distance between spatial quantiles of order $\alpha \to 1$ in direction u and the half-line $\{m + ru : r \geq 0\}$ converges to zero, that is, it may be so that these extreme quantiles are not eventually on the half-line with direction u originating from the spatial median m; see Figure 1(a)–(b) in Paindaveine and Virta (2021)

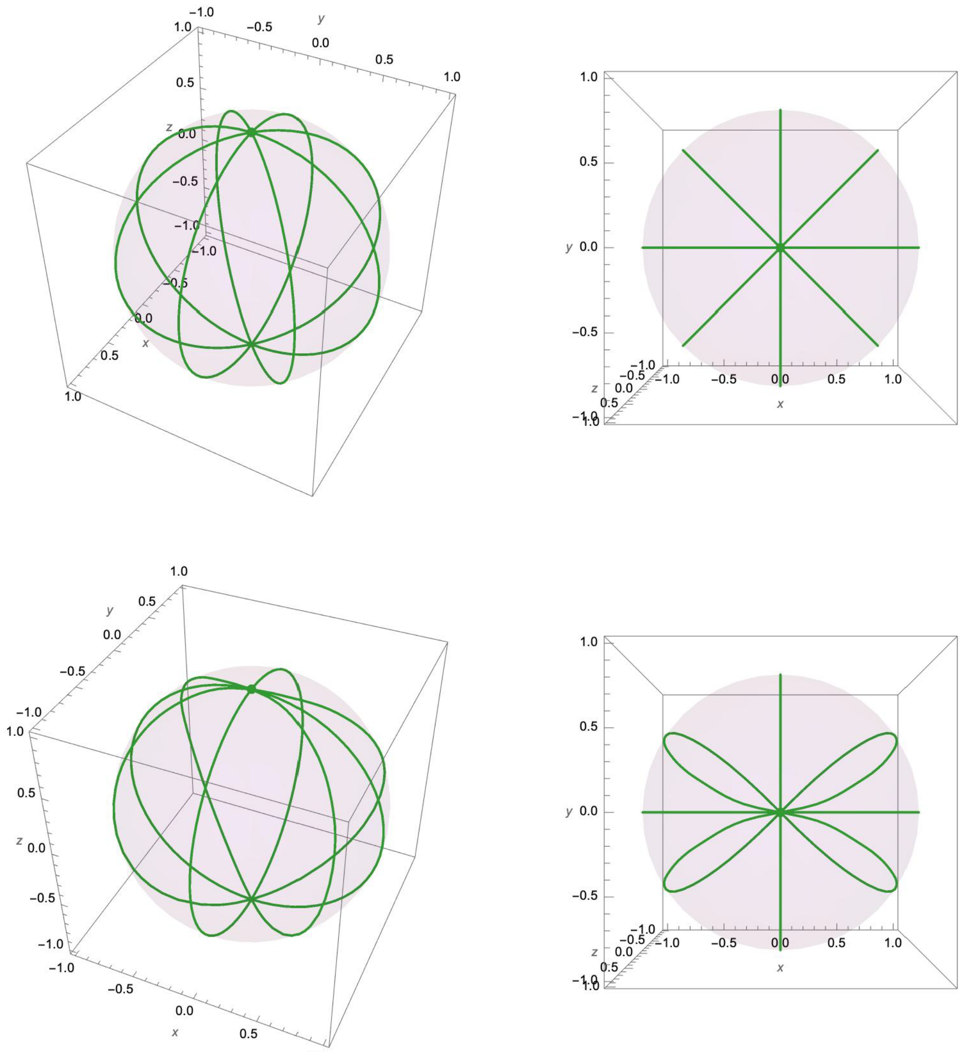

FIG. 1. *Quantile curves* $\alpha(\in[0,1]) \mapsto \mu^m_{\alpha,u}$ *in each of the eight directions* $u = (\cos(k\pi/4), \sin(k\pi/4), 0)$, $k = 0, 1, \dots, 7$, *for the rotationally symmetric probability measure* (P_1) *and the nonrotationally symmetric one* (P_2) *described in the last paragraph of Section* 3.1 (*top and bottom row, respectively*); *in each case, the second column offers a view from above the Fréchet median* m, *that is marked as a green dot.*

for examples. Interestingly, the spherical result in Theorem 3.3(ii) is thus stronger than the corresponding Euclidean result.

We conclude this section with a graphical illustration for $d = 3$; see Figure 1. We consider the von Mises–Fisher distribution with location $\theta = (0, 0, 1)$ and concentration $\kappa = 1$, that is, the distribution, P_1 say, of

$$X = Z\theta + \sqrt{1 - Z^2}\begin{pmatrix} S \\ 0 \end{pmatrix},$$

where Z and S are mutually independent, Z admits the density $z \mapsto c_\kappa \exp(\kappa z)\mathbb{I}[-1 \le z \le 1]$ with respect to the Lebesgue measure (c_κ is a normalizing constant), and S is uniformly distributed over $\mathcal{S}^1$. We also consider the probability measure P_2 obtained when S rather results from projecting radially onto $\mathcal{S}^1$ a bivariate normal random vector with mean zero and covariance matrix $\Sigma = \mathrm{diag}(25, 1)$ (in the terminology of Tyler (1987), S thus follows an *angular Gaussian distribution* with a shape matrix proportional to Σ). Both for $\ell = 1$

and $\ell = 2$, Figure 1 then draws the quantile curves $\alpha(\in [0,1]) \mapsto \mu^m_{\alpha,u}(P_\ell)$ in each of the eight directions $u = (\cos(k\pi/4), \sin(k\pi/4), 0)$, $k = 0, 1, \ldots, 7$. In the rotationally symmetric setup $\ell = 1$, these quantile curves are geodesics (great half-circles) from m to $-m$, which actually illustrates Theorem 5.1 below. For $\ell = 2$, quantile curves are geodesics for $k = \{0, 2, 4, 6\}$ only, and the four other quantile curves are not contained in a plane, which reflects the nonrotational symmetry of this probability measure.

3.2. *The spherical quantile function.* The results of the previous section allow us to formally define the spherical quantile function associated with our quantile concept and to study some of its properties. For any $\mu \in \mathcal{S}^{d-1}$ and any $r \in (0, 1]$, let $\mathcal{B}_{\mu,r} = \{z \in T_\mu\mathcal{S}^{d-1} : \|z\| < r\}$ and $\mathcal{B}^\infty_{\mu,r} := \mathcal{B}_{\mu,r} \cup \{u^\infty_{\mu,r}\}$, where $u^\infty_{\mu,r}$ is a single element identifying all points in the closed annulus $\overline{\mathcal{B}_{\mu,1}} \setminus \mathcal{B}_{\mu,r}$ (here, $\bar{A}$ is the closure of A with respect to the usual topology). We endow the space $\mathcal{B}^\infty_{\mu,r}$ with the metric $\delta_{\mu,r}$ defined by

$$\delta_{\mu,r}(z_1, z_2) := \begin{cases} \|z_1 - z_2\| & \text{if } z_1, z_2 \in \mathcal{B}_{\mu,r} \\ r - \|z_1\| & \text{if } z_1 \in \mathcal{B}_{\mu,r} \text{ and } z_2 = u^\infty_{\mu,r} \\ r - \|z_2\| & \text{if } z_1 = u^\infty_{\mu,r} \text{ and } z_2 \in \mathcal{B}_{\mu,r} \\ 0 & \text{if } z_1 = z_2 = u^\infty_{\mu,r} \end{cases}$$

(it is easy to check that $\delta_{\mu,r}$ is a proper metric on $\mathcal{B}^\infty_{\mu,r}$). The corresponding norm on $\mathcal{B}^\infty_{\mu,r}$ is then defined through $\|z\|_{\mu,r} := \delta_{\mu,r}(0, z)$. Elements of $\mathcal{B}^\infty_{\mu,r}$ that belong to $\mathcal{B}_{\mu,r}$ will often be written as $z = \alpha u$, where $\alpha \in [0, r)$ and u is a unit vector of $T_\mu\mathcal{S}^{d-1}$. The quantile function is then formally defined as follows.

DEFINITION 3.1. Fix $P \in \mathcal{P}_{d-1}$, with $d \geq 3$, and let m be the Fréchet median of P. Assume that P is not concentrated on a great circle containing m. Then the m-quantile function of P is the map

$$Q = Q^m_P : \mathcal{B}^\infty_{m,p_m} \to \mathcal{S}^{d-1}$$

defined through $Q(\alpha u) = \mu^m_{\alpha,u}$ for $\alpha u \in \mathcal{B}_{m,p_m}$ and $Q(u^\infty_{m,p_m}) = -m$.

This definition is motivated by the fact that $\mu^m_{\alpha,u} = -m$ for any $\alpha \in [p_m, 1]$ and any unit vector $u \in T_m\mathcal{S}^{d-1}$ (see Definition 2.2), so that identifying all points in the closed annulus $\overline{\mathcal{B}_{m,1}} \setminus \mathcal{B}_{m,p_m}$ to u^∞_{m,p_m} leads to the above definition. Observe that, in the important case where $-m$ is not an atom of P, $u^\infty_{m,p_m} = u^\infty_{m,1}$ simply identifies the points in the boundary of $\mathcal{B}_{m,1}$, that is, those belonging to the unit sphere in $T_m\mathcal{S}^{d-1}$.

We turn to continuity of Q. We did not define the quantile function in the circular case $d = 2$, as our assumption that guarantees uniqueness of quantiles is never satisfied on the circle (for $d = 2$, the unit circle is itself a great circle through m that will always have P-probability one). Yet, a circular quantile function could similarly be defined once a convention has been taken to identify a unique quantile, such as, for example, the classical infimum-based one in the univariate Euclidean case. The resulting circular quantile function may of course fail to be continuous (in particular, it will not be continuous for empirical probability measures). In contrast, for $d \geq 3$, the quantile function is continuous for any probability measure P, even for an empirical probability measure P. We have the following result.

THEOREM 3.4. *Fix $P \in \mathcal{P}_{d-1}$, with $d \geq 3$, and let m be the Fréchet median of P. Assume that P is not concentrated on a great circle containing m. Then the quantile function $Q = Q^m_P : \mathcal{B}^\infty_{m,p_m} \to \mathcal{S}^{d-1}$ is continuous (here, $\mathcal{B}^\infty_{m,p_m}$ is equipped with the metric δ_{m,p_m}).*

We will later show that, for any probability measure P on $\mathcal{S}^{d-1}$, with $d \geq 3$, that is not concentrated on a great circle containing m, the quantile function $Q_P^m : \mathcal{B}_{m,p_m}^{\infty} \to \mathcal{S}^{d-1}$ is actually surjective and that it may fail to be injective for atomic probability measures only; see Theorem 4.4. These further results, as well as the important result stating that the quantile function characterizes the underlying probability measure, require the spherical rank concept that will be introduced in the next section.

4. Gradient conditions and spherical ranks. The main goal of this section is to introduce a *spherical rank function*, that under mild assumptions on the underlying probability measure, will be the inverse map of the spherical quantile function considered above. As we will see, this rank function is the right tool to obtain further results on the quantile function. The rank function is intimately linked to the gradient condition associated with the spherical quantiles $\mu_{\alpha,u}^m(P)$, a gradient condition that itself will follow from the directional derivatives of the objective function $M_{\alpha,u}^{m,P}$ defining these quantiles; see Definition 2.2.

THEOREM 4.1. *Fix $P \in \mathcal{P}_{d-1}$, with $d \geq 3$, and let m be the Fréchet median of P. Fix $\alpha \in [0, p_m)$ (still with $p_m := 1 - P[\{-m\}]$) and a unit vector $u \in T_m\mathcal{S}^{d-1}$. Fix $\mu \in \mathcal{S}_{-m}^{d-1}$ and a unit vector v in $T_\mu\mathcal{S}^{d-1}$. Let $\varphi : [0, \pi] \to \mathcal{S}^{d-1}$ be a geodesic path such that $\varphi(0) = \mu$ and $\dot{\varphi}(0) = v$. Then the directional derivative*

$$\frac{\partial M_{\alpha,u}^{m,P}}{\partial v}(\mu) = \lim_{t \overset{>}{\to} 0} \frac{M_{\alpha,u}^{m,P}(\varphi(t)) - M_{\alpha,u}^{m,P}(\mu)}{t} \tag{4.1}$$

exists and is given by

$$\begin{aligned}\frac{\partial M_{\alpha,u}^{m,P}}{\partial v}(\mu) = {} & \frac{1}{p_m}\big(d\pi_m(\mu)v\big)'\bigg\{p_m \mathrm{E}\bigg[\frac{\pi_m(\mu) - \pi_m(X)}{\|\pi_m(\mu) - \pi_m(X)\|}\xi_{X,\mu}\bigg] - \alpha u\bigg\} \\ & + \frac{1}{p_m}\|d\pi_m(\mu)v\| P[\{\mu\}],\end{aligned}$$

where X is an $\mathcal{S}_{-m}^{d-1}$-valued random vector with distribution P_{-m} and where we let $\xi_{x,y} = \mathbb{I}[x \neq y]$. Above, $d\pi_m(\mu) : T_\mu\mathcal{S}^{d-1} \to T_m\mathcal{S}^{d-1}$ is the differential of the map $\pi_m : \mathcal{S}_{-m}^{d-1} \to T_m\mathcal{S}^{d-1}$ in (2.2) (we refer to Lemma S.4.1 for an explicit expression).

For $\alpha \in [0, p_m)$ and a unit vector u in $T_m\mathcal{S}^{d-1}$, any m-quantile of order α in direction u by definition belongs to $\mathcal{S}_{-m}^{d-1}$ and minimizes the objective function $M_{\alpha,u}^{m,P}$ over $\mathcal{S}_{-m}^{d-1}$. As we will show in Lemma S.4.2, $\mu (\in \mathcal{S}_{-m}^{d-1})$ is an m-quantile of order α in direction u for P *if and only if* the directional derivative in (4.1) is nonnegative for any unit vector v in $T_\mu\mathcal{S}^{d-1}$. Theorem 4.1 then allows us to obtain the gradient condition provided in the following result.

THEOREM 4.2. *Fix $P \in \mathcal{P}_{d-1}$, with $d \geq 3$, and let m be the Fréchet median of P. Fix $\alpha \in [0, p_m)$ and a unit vector u in $T_m\mathcal{S}^{d-1}$. Then $\mu (\in \mathcal{S}_{-m}^{d-1})$ is an m-quantile of order α in direction u for P if and only if*

$$\bigg\| p_m \mathrm{E}\bigg[\frac{\pi_m(\mu) - \pi_m(X)}{\|\pi_m(\mu) - \pi_m(X)\|}\xi_{X,\mu}\bigg] - \alpha u\bigg\| \leq P[\{\mu\}], \tag{4.2}$$

where X is an $\mathcal{S}_{-m}^{d-1}$-valued random vector with distribution P_{-m}.

Fix $\mu \in \mathcal{S}_{-m}^{d-1}$, $\alpha \in [0, p_m)$ and a unit vector u in $T_m\mathcal{S}^{d-1}$, and assume that P is not concentrated on a great circle containing m, so that $\mu_{\alpha,u}^m = Q(\alpha u)$ is unique (Theorem 3.1). Denoting for a moment the quantity inside the norm in (4.2) as $R(\mu) - \alpha u$, Theorem 4.2 shows that $R(\mu) = \alpha u$ implies $\mu = Q(\alpha u)$. Thus, the resulting function R is a natural candidate to be the inverse map of Q. We adopt the following definition.

DEFINITION 4.1. Fix $P \in \mathcal{P}_{d-1}$, with $d \geq 3$, and let m be the Fréchet median of P. Assume that P is not concentrated on a great circle containing m. Let X be an $\mathcal{S}^{d-1}_{-m}$-valued random vector with distribution P_{-m}. Then the rank function of P is the map $R = R^m_P : \mathcal{S}^{d-1} \to \mathcal{B}^\infty_{m,p_m}$ such that

$$R(\mu) = p_m \mathrm{E}\left[\frac{\pi_m(\mu) - \pi_m(X)}{\|\pi_m(\mu) - \pi_m(X)\|}\xi_{X,\mu}\right] \tag{4.3}$$

for $\mu \in \mathcal{S}^{d-1}_{-m}$ and $R(-m) = u^\infty_{m,p_m}$.

In the framework of this definition, Lemma S.1.3 and Corollary S.1.1 together entail that the distribution of $\pi_m(X)$ is not concentrated on a line of $\mathbb{R}^d$, so that the proof of Proposition 2.1 in Girard and Stupfler (2017) ensures that $\|R(\mu)\| < p_m$ for any $\mu \in \mathcal{S}^{d-1}_{-m}$; this justifies that the rank function R indeed takes its values in $\mathcal{B}^\infty_{m,p_m}$ and, less importantly, this also shows that $-m$ is the only location on the sphere that is given rank u^∞_{m,p_m}. Like the quantile function defined in the previous section, the rank function is then always continuous for $d \geq 3$.

THEOREM 4.3. *Fix $P \in \mathcal{P}_{d-1}$, with $d \geq 3$, and let m be the Fréchet median of P. Assume that P is not concentrated on a great circle containing m. Then the rank function $R = R^m_P : \mathcal{S}^{d-1} \to \mathcal{B}^\infty_{m,p_m}$ is continuous (again, $\mathcal{B}^\infty_{m,p_m}$ is equipped with the metric δ_{m,p_m}).*

By using this rank function, we can show that the quantile function $Q = Q^m_P$ is always a surjective map from $\mathcal{B}^\infty_{m,p_m}$ to $\mathcal{S}^{d-1}$ and that, under the further assumption that P is nonatomic, Q is a one-to-one map, whose inverse map is the corresponding rank function R. More precisely, we have the following result.

THEOREM 4.4. *Fix $P \in \mathcal{P}_{d-1}$, with $d \geq 3$, and let m be the Fréchet median of P. Assume that P is not concentrated on a great circle containing m. Then: (i) $Q^m_P : \mathcal{B}^\infty_{m,p_m} \to \mathcal{S}^{d-1}$ is a surjective map; (ii) If P is also nonatomic, then $Q^m_P : \mathcal{B}^\infty_{m,p_m} \to \mathcal{S}^{d-1}$ is a homeomorphism, with inverse given by $R^m_P : \mathcal{S}^{d-1} \to \mathcal{B}^\infty_{m,p_m}$.*

A corollary of Theorem 4.4(i) is that, under the extremely mild assumptions of this result, the Euclidean spatial quantiles in $T_m\mathcal{S}^{d-1}$, that are pulled back to generate our spherical spatial quantiles $\mu^m_{\alpha,u}$, for any $\alpha \in [0, p_m)$ and any unit vector $u \in T_m\mathcal{S}^{d-1}$, do fill the whole tangent space $T_m\mathcal{S}^{d-1}$. A direct consequence is that, while there was some flexibility on the choice of the projection π_m when defining our spherical quantiles in Section 2.2, this projection had to be a *one-to-one* map from $\mathcal{S}^{d-1}_{-m}$ to $T_m\mathcal{S}^{d-1}$. Arguably, the stereographic projection is the most classical projection meeting this key requirement, a requirement that in particular excludes the Riemannian log map at m since this map is a one-to-one map from $\mathcal{S}^{d-1}_{-m}$ to a bounded open disk in $T_m\mathcal{S}^{d-1}$.

As the following result shows, the rank function $R = R^m_P$ actually characterizes the probability measure P, so that, under the assumptions that guarantee that the quantile and rank functions are inverse maps of one another, the quantile function also characterizes the underlying probability measure.

THEOREM 4.5. *(i) Assume that $P_1, P_2 \in \mathcal{P}_{d-1}$ share the same Fréchet median m and are not concentrated on a great circle containing m. Then $R^m_{P_1} = R^m_{P_2}$ if and only if $P_1 = P_2$. (ii) Assume further that P_1 and P_2 are nonatomic. Then $Q^m_{P_1} = Q^m_{P_2}$ if and only if $P_1 = P_2$.*

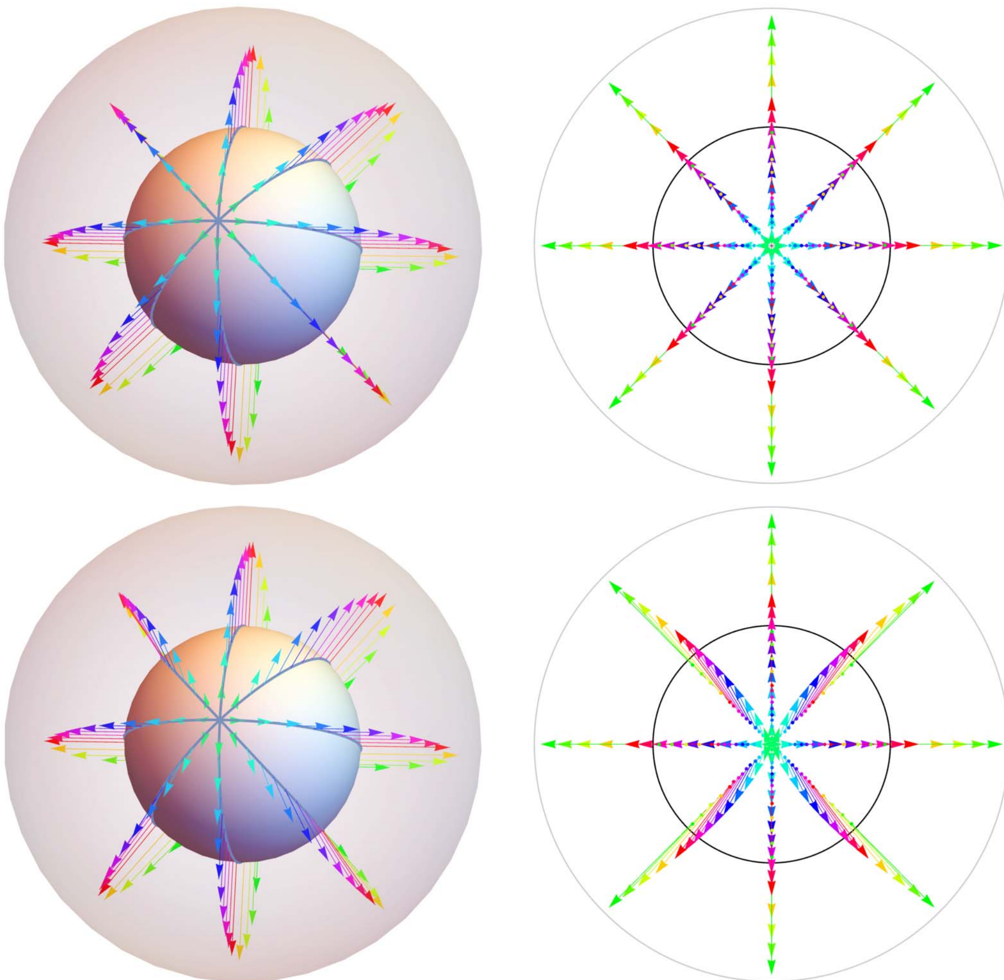

FIG. 2. *Ranks* $R^m_{P_\ell}(\mu)$ *associated with* 15 *locations* μ *on each of the* 8 *geodesics* $\{(\cos\varphi)\theta + (\sin\varphi)u : \varphi \in [0,\pi]\}$ *associated with* $u = (\cos(k\pi/4), \sin(k\pi/4), 0)$, $k = 0, 1, \ldots, 7$. *Ranks, that are of the form* $\alpha u = \alpha(u_1, u_2, 0)$, *here are drawn as arrows with length* α *and direction* u *located at the* 15×8 *points* $\mu = (\cos\varphi)\theta + (\sin\varphi)u$ *considered in* $\mathcal{S}^2$ *(left panels) or as arrows with length* α *and direction* (u_1, u_2) *located at the corresponding points* $\varphi(u_1, u_2)$ *in* $\mathbb{R}^2$ *(right panels); the top and bottom rows correspond to the rotationally symmetric probability measure* (P_1) *and the nonrotationally symmetric one* (P_2) *already considered in Figure* 1, *respectively.*

Inspection of the proof of Theorem 4.5(i) reveals that the result actually does not require the assumption that distributions are not concentrated on any great circle containing m (in such a case, rank functions are still defined as in Definition 4.1, but they are no longer guaranteed to take their values in $\mathcal{B}^\infty_{m,p_m}$). This assumption, however, cannot be dropped in Theorem 4.5(ii) since quantile functions are not properly defined when this assumption is violated.

Figure 2 provides a graphical illustration of the proposed spherical ranks for the probability measures P_1 and P_2 already considered in Figure 1. More precisely, the figure represents the spherical ranks $R^m_{P_\ell}(\mu)$ associated with 15 locations μ on each of the 8 geodesics $\{(\cos\varphi)\theta + (\sin\varphi)u : \varphi \in [0,\pi]\}$ associated with $u = (\cos(k\pi/4), \sin(k\pi/4), 0)$, $k = 0, 1, \ldots, 7$. For easier visualization, these ranks that take values of the form $\alpha u = \alpha(u_1, u_2, 0)$ in $B^\infty_{m,1}$ (recall that $m = \theta = (0, 0, 1)$) are both drawn as arrows with length α and direction u located at the 15×8 points $\mu = (\cos\varphi)\theta + (\sin\varphi)u$ considered in $\mathcal{S}^2$ (left panels) or as arrows with length α and direction (u_1, u_2) located at the corresponding points $\varphi(u_1, u_2)$ in $\mathbb{R}^2$ (right panels). These ranks are to be thought of as the duals of the quantiles in Figure 1: they give, along each of the corresponding geodesics, the order α and direction u for which the proposed spherical quantile is the given point on the geodesic. As expected, the norm of $R^m_{P_\ell}(\mu)$ converges to one as μ converges to $-m$. Clearly, ranks have the same direction as the corresponding geodesic for the rotationally symmetric distribution P_1, but this is the case only for half of the geodesics considered for P_2.

5. Spherical depth. If a location μ on the unit sphere is an m-quantile of order α in direction u for the probability measure P at hand, then the larger α is, the more outlying μ is with respect to P. In other words, $\alpha = \|R(\mu)\|_{m,p_m}$ measures the *outlyingness* of μ with respect to P (here, $\|\cdot\|_{m,p_m}$ is the norm defined in Section 3.2). Thus, $1 - \|R(\mu)\|_{m,p_m}$ is a measure of centrality of μ with respect to P, which leads to the following definition.

DEFINITION 5.1. Fix $P \in \mathcal{P}_{d-1}$, with $d \geq 3$, and let m be the Fréchet median of P. Assume that P is not concentrated on a great circle containing m. Then the depth function of P is the map $D = D^m_P : \mathcal{S}^{d-1} \to [1 - p_m, 1]$ such that $D(\mu) = 1 - \|R(\mu)\|_{m,p_m}$ for any $\mu \in \mathcal{S}^{d-1}$ (recall that, by definition, $\|R(-m)\|_{m,p_m} = \|u^\infty_{m,p_m}\|_{m,p_m} = p_m$).

For any $d \geq 3$, the depth function D^m_P is continuous over $\mathcal{S}^{d-1}$ as soon as P is not concentrated on a great circle containing m (this is a direct corollary of Theorem 4.3). Thus, if μ diverges to "infinity" (with respect to m), that is, if it converges to $-m$, then $D^m_P(\mu)$ converges to $1 - p_m$. This is somewhat in contrast to depth functions in Euclidean spaces, for which a classical requirement is that the depth of μ converges to zero as $\|\mu\|$ diverges to infinity; see Property P4 in Zuo and Serfling (2000). This "vanishing at infinity" property is a natural requirement indeed in Euclidean spaces since such spaces cannot contain probability mass at infinity. We argue that since, in contrast, spheres may have an atom at $-m$, it is also natural that the depth does not vanish at $-m$ in such cases. We stress, however, that in the important case $p_m = 1$ where there is no atom at $-m$, then the proposed spherical depth is indeed vanishing at infinity, which is quite natural—interestingly, recent proposals for depth on general metric spaces actually rather impose this vanishing at infinity for unbounded spaces only; see, for example, Dai and Lopez-Pintado (2023).

In the same line of thought, note that the proposed spherical depth could in principle be equal to zero, that is, in the case $p_m = 1$ (when there is not atom at $-m$). Nevertheless, the properties of the rank function entail that zero depth will be achieved at $-m$ only. In other words, irrespective of the probability measure P at hand, our depth has the "nonvanishing property" in the sense that it is strictly positive over $\mathcal{S}^{d-1}_{-m}$. This is a very desirable property in some inferential applications; we refer to Section 7.1 for an example.

Now, for any depth function, be it in a Euclidean space or a non-Euclidean one, it is natural to consider the corresponding depth regions, that collect the locations μ with a depth that is larger than or equal to a given order α. In other words, the α-depth region is

$$\mathcal{R}^m_P(\alpha) := \{\mu \in \mathcal{S}^{d-1} : D^m_P(\mu) \geq \alpha\},$$

and the corresponding depth contour is then the boundary, $\mathcal{C}^m_P(\alpha) := \partial\mathcal{R}^m_P := \{\mu \in \mathcal{S}^{d-1} : D^m_P(\mu) = \alpha\}$ of this depth region. Obviously, depth regions form a collection of nested subsets of the unit sphere $\mathcal{S}^{d-1}$, the innermost, $\mathcal{R}^m_P(1)$, being $\{m\}$, and the outermost, $\mathcal{R}^m_P(1 - p_m)$, being the sphere itself. The shape of depth contours reflects the "structure" of the underlying probability measure. In particular, we have the following result.

THEOREM 5.1. *Fix $P \in \mathcal{P}_{d-1}$, with $d \geq 3$, and let m be the Fréchet median of P. Assume that P is rotationally symmetric about m. Then*: (*i*) *for $\alpha = 0$ and any unit vector $u \in T_m\mathcal{S}^{d-1}$, the unique m-quantile $\mu^m_{\alpha,u}$ is m*; (*ii*) *for any $\alpha \in [0, 1]$ and any unit vector $u \in T_m\mathcal{S}^{d-1}$, the* *unique m-spatial quantile $\mu^m_{\alpha,u}$ belongs to the meridian $\{(\cos t)m + (\sin t)u : t \in [0, \pi]\}$; (iii) for any unit vector $u \in T_m\mathcal{S}^{d-1}$, the map $\alpha \mapsto d(\mu^m_{\alpha,u}, m)$ is monotone nondecreasing over $[0, 1]$; (iv) when P is not concentrated on $\{-m, m\}$, each depth contour $\mathcal{C}^m_P(\alpha)$ is of the form $\{\mu \in \mathcal{S}^{d-1} : \mu'm = c_\alpha\}$, and the map $\alpha \mapsto c_\alpha$ is monotone nondecreasing.*

A key ingredient in the proof of Theorem 5.1 is the following rotation-equivariance result for spherical quantiles, which is of independent interest.

THEOREM 5.2. *Fix $P \in \mathcal{P}_{d-1}$, with $d \geq 3$, and let m be the Fréchet median of P. Let O be a $d \times d$ orthogonal matrix such that $Om = m$ and denote as P_O the distribution of OX when X has distribution P. Fix $\alpha \in [0, 1]$ and a unit vector u in $T_m\mathcal{S}^{d-1}$. Then μ is an m-quantile of order α in direction u for P if and only if $O\mu$ is an m-quantile of order α in direction Ou for P_O.*

We stress that, in Theorem 5.1(ii), m may be an m-spatial quantile of order $\alpha > 0$ in direction u, provided that m is an atom of P. Actually, it is easy to prove that the largest α for which m is an m-spatial quantile of order α in (any) direction u is $P[\{m\}]$. More importantly, Theorem 5.1(iv) shows that a probability measure P that is rotationally symmetric about m provides depth contours that are themselves invariant under rotations fixing m; of course, this is also the case for the corresponding depth regions, that are spherical caps centered at m. Departures from rotational symmetry will result into depth regions that exhibit other shapes, which is an advantage over the depth regions from Ley, Sabbah and Verdebout (2014) that are "concentric" spherical caps even for probability measures that are not rotationally symmetric. This is illustrated in Figure 3 that draws the depth contours $C^m_P(\alpha)$, $\alpha = 0, 0.2, 0.4, 0.6, 0.8$, for both probability measures that were considered in Figures 1–2.

6. Asymptotics. In the sample case, evaluation of our spherical quantiles requires estimating the population Fréchet median, and we therefore start this section by providing results that describe the asymptotic behavior of sample Fréchet medians. When a random sample $X_1, \dots, X_n$ from P is available, a sample Fréchet median is defined as a Fréchet median of the corresponding empirical probability measure P_n, that is, as a minimizer of

$$\mu \mapsto \frac{1}{n}\sum_{i=1}^{n} d(\mu, X_i) = \frac{1}{n}\sum_{i=1}^{n} \arccos(\mu' X_i)$$

over $\mathcal{S}^{d-1}$. If P admits a density with respect to the surface area measure on $\mathcal{S}^{d-1}$, then such a sample Fréchet median is almost surely unique; see Theorem 4.15 from Yang (2011). We then have the following almost sure consistency and Bahadur representation results.

THEOREM 6.1. *Fix $P \in \mathcal{P}_{d-1}$, with $d \geq 3$, and let m be the Fréchet median of P. Let $X_1, X_2, \dots$ be mutually independent random vectors with distribution P, and let $\hat{m}_n$ be an arbitrary sample Fréchet median associated with $X_1, \dots, X_n$. Then*:

$$(i) \quad \hat{m}_n \to m \quad \text{almost surely}$$

as n diverges to infinity. (ii) Assuming further that P admits a bounded density with respect to the surface area measure on $\mathcal{S}^{d-1}$ and that

$$K := \mathrm{E}\bigg[\frac{m'X_1}{\|(I_d - mm')X_1\|}\bigg(I_d - \frac{(I_d - mm')X_1X_1'(I_d - mm')}{\|(I_d - mm')X_1\|^2}\bigg)\xi_{X_1,\pm m}\bigg]$$

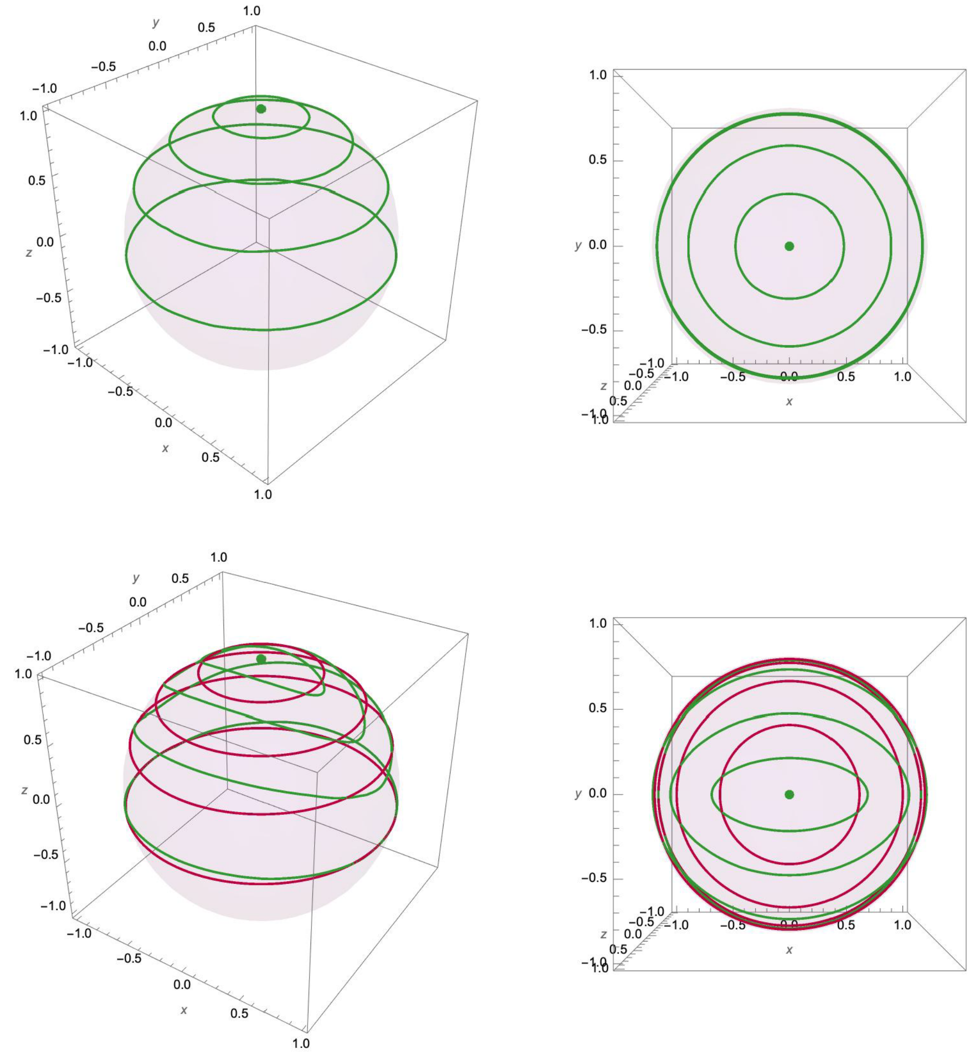

FIG. 3. *Depth contours $C_P^m(\alpha)$, $\alpha = 0, 0.2, 0.4, 0.6, 0.8$, computed from the first probability measure (top row) and second one (bottom row) in Figure 1; in each case, the second column offers a view from above the Fréchet median, that is marked as a green dot. In the bottom row, the quantile contours from Ley, Sabbah and Verdebout (2014) containing the same probability mass as the proposed contours are plotted in red (these are not plotted in the top row since, in the rotationally symmetric setup considered there, those contours coincide with the proposed ones).*

exists, is finite, and is invertible, where we let $\xi_{x,\pm y} := \mathbb{I}[x \notin \{\pm y\}]$, we have

$$\sqrt{n}(\hat{m}_n - m) = K^{-1} \frac{1}{\sqrt{n}} \sum_{i=1}^{n} \frac{(I_d - mm')X_i}{\|(I_d - mm')X_i\|} \xi_{X_i,\pm m} + o_{\mathrm{P}}(1) \tag{6.1}$$

as n diverges to infinity.

Because it concerns the Fréchet median, this asymptotic result of course intersects with results already available in the literature. In particular, the consistency result in Theorem 6.1(i) is essentially the one obtained in Theorem 2.3 from Bhattacharya and Patrangenaru (2003), where a much more general metric space was considered (for the sake of completeness, we still provide in Section S.6 a simple proof, that exploits compactness and separability of the sample space we consider). The Bahadur representation result in Theorem 6.1(ii) readily yields an asymptotic normality result that was obtained, under slightly more stringent assumptions, in Bhattacharya and Lin (2017); see also Kendall and Le (2011) and Eltzner and Huckemann (2019). While the proofs of asymptotic normality in some of these papers are based on Bahadur representation results, the result in (6.1) has the advantage to involve population and sample quantities on the sphere rather than their coordinates in a flat space, which will be useful to deduce, from Theorem 6.2(ii) below, an explicit asymptotic normality result for higher-order sample spherical quantiles.

More importantly, we now turn indeed to higher-order sample spherical quantiles, which for the problem of estimating $\mu^m_{\alpha,u}$, with given $\alpha \in (0,1]$ and $u \in T_m\mathcal{S}^{d-1}$, are defined as follows. Assuming again that a random sample $X_1,\dots,X_n$ from a probability measure P is available, we first estimate m by the sample Fréchet median $\hat{m}_n$ of $X_1,\dots,X_n$. Since quantiles with respect to $\hat{m}_n$ should involve a direction that is a unit vector in $T_{\hat{m}_n}S^{d-1}$, we then consider an arbitrary (possibly random) sequence (u_n), with $u_n \in T_{\hat{m}_n}\mathcal{S}^{d-1}$ for any n, such that $(u_n) \to u$ almost surely as $n \to \infty$; practical choices for such a sequence (u_n) will be discussed below. For $\alpha \in (0,1)$, this naturally leads to the sample quantile $\hat{\mu}^{\hat{m}_n}_{\alpha,u_n}$ defined as the minimizer of the function

$$\mu \mapsto \frac{1}{n}\sum_{i=1}^{n}\{\|\pi_{\hat{m}_n}(X_i) - \pi_{\hat{m}_n}(\mu)\| - \|\pi_{\hat{m}_n}(X_i)\| - \alpha u_n'\pi_{\hat{m}_n}(\mu)\}$$

over $\mathcal{S}^{d-1}_{-\hat{m}_n}$. According to Theorem 3.1(ii), uniqueness is guaranteed as soon as the X_i's do not belong to a common great circle containing $\hat{m}_n$, hence in particular holds almost surely in the framework of Theorem 6.2(ii) below. Of course, for $\alpha = 1$, we simply put $\hat{\mu}^{\hat{m}_n}_{\alpha,u_n} := -\hat{m}_n$. We then have the following almost sure consistency and Bahadur representation results.

THEOREM 6.2. *Fix $P \in \mathcal{P}_{d-1}$, with $d \geq 3$, let m be the Fréchet median of P. Assume that* $\mathrm{P}[\{-m,m\}] = 0$ *and that P is not concentrated on a great circle containing m. Let $X_1, X_2, \dots$ be mutually independent random vectors with distribution P, and let $\hat{m}_n$ be an arbitrary sample Fréchet median associated with $X_1,\dots,X_n$. Fix $\alpha \in (0,1)$, $u \in T_m\mathcal{S}^{d-1}$, and an arbitrary (possibly random) sequence (u_n), with $u_n \in T_{\hat{m}_n}S^{d-1}$ for any n, such that $(u_n) \to u$ almost surely as n diverges to infinity. Then letting, for any n, $\hat{\mu}^{\hat{m}_n}_{\alpha,u_n}$ be an arbitrary $\hat{m}_n$-spatial quantile of order α in direction u_n,*

$$\hat{\mu}^{\hat{m}_n}_{\alpha,u_n} \to \mu^m_{\alpha,u} \quad \textit{almost surely}$$

as n diverges to infinity. (*ii*) *Assuming further that the assumptions of Theorem 6.1(ii) hold, we have*

$$\begin{aligned}\sqrt{n}(\hat{\mu}^{\hat{m}_n}_{\alpha,u_n} - \mu^m_{\alpha,u}) &= (m'\mu^m_{\alpha,u})\sqrt{n}(\hat{m}_n - m) \\ &\quad - J_q(\pi_m^{-1})V^{-1}\frac{1}{\sqrt{n}}\sum_{i=1}^{n}\left(\frac{\pi_m(X_i)-q}{\|\pi_m(X_i)-q\|}\xi_{\pi_m(X_i),q} + \alpha u\right) + o_{\mathrm{P}}(1)\end{aligned} \tag{6.2}$$

as n diverges to infinity, where we let

$$V := \mathrm{E}\left[\frac{1}{\|\pi_m(X)-q\|}\left(I_d - \frac{(\pi_m(X)-q)(\pi_m(X)-q)'}{\|\pi_m(X)-q\|^2}\right)\xi_{\pi_m(X),q}\right]$$

and where $J_q(\pi_m^{-1})$ stands for the Jacobian matrix of π_m^{-1} at $q := \pi_m(\mu^m_{\alpha,u})$.

Some comments are in order. First, note that we do not consider the particular cases $\alpha = 0$ and $\alpha = 1$ in Theorem 6.2, as the corresponding sample quantiles are then equal to $\hat{m}_n$ (by Theorem 3.2) and $-\hat{m}_n$ (by definition), hence have an asymptotic behavior that directly results from Theorem 6.1. Second, in the Bahadur representation (6.2), the first term of the right-hand side is associated with the estimation of the Fréchet median m, whereas the second term corresponds to spherical quantile estimation.[4] Third, Ley, Sabbah and Verdebout (2014) also obtained a two-term Bahadur representation of this form for their spherical cap quantiles, and they actually showed that the first term vanishes under rotational symmetry (see their Proposition 3.2). In contrast, rotational symmetry will not put to zero the first term in the right-hand side of (6.2), which is due to the fact that the directional (in u) nature of our quantiles breaks the underlying symmetry. Fourth and last, an asymptotic normality result for $\sqrt{n}(\hat{\mu}^{\hat{m}_n}_{\alpha,u_n} - \mu^m_{\alpha,u})$, with an explicit asymptotic covariance matrix, can of course readily be obtained from Theorems 6.1(ii) and 6.2(ii).

We end this section by discussing how to choose in practice the direction sequence (u_n). One possible choice is obtained by fixing a given target location $\mu \in \mathcal{S}^{d-1}$ and by considering, for any n, the direction u_n pointing to μ from $\hat{m}_n$, that is, the unit vector $u_n = U_\mu(\hat{m}_n) \in T_{\hat{m}_n}\mathcal{S}^{d-1}$ such that the geodesic from $\hat{m}_n$ to μ is $\{(\cos t)\hat{m}_n + (\sin t)u_n : t \in [0, d(\hat{m}_n, \mu)]\}$. This scheme, that identifies a unique direction u_n as soon as $\hat{m}_n \in \mathcal{S}^{d-1} \setminus \{\pm\mu\}$, provides a sequence (u_n) converging to $u = U_\mu(m) \in T_m\mathcal{S}^{d-1}$. While targeting a fixed location indeed bears a clear directional meaning in practice, another appealing way to match directions associated with different tangent spaces is to use parallel transport. In the present context, this consists in picking some $u_N \in T_{\hat{m}_N}\mathcal{S}^{d-1}$ for some given sample size N, and then in obtaining u_{N+k}, $k = 1, 2, \dots$ by iteratively transporting in a parallel way u_{N+k-1} from the tangent space at $\hat{m}_{N+k-1}$ to the tangent space at $\hat{m}_{N+k}$. While this may seem natural at first sight, the resulting sequence (u_n) does not converge almost surely to a limiting direction $u \in T_m\mathcal{S}^{d-1}$, since the pathwise limit of $(u_n(\omega))$ will depend on the path of $(\hat{m}_n(\omega))$ and not only on its path-independent limit m.

7. Two applications. In this section, we illustrate the practical relevance of the proposed hyperspherical concepts by considering two inferential applications, namely supervised classification (Section 7.1) and testing for rotational symmetry (Section 7.2).

7.1. *Supervised classification.* One of the most successful applications of statistical depth in the last two decades is supervised classification, based on the "max-depth" approach; see, among many others, Ghosh and Chaudhuri (2005) and Li, Cuesta-Albertos and Liu (2012). This approach classifies an observed location $\mu = x$ as generated from a probability measure P_1 rather than P_2 if the depth of x with respect to P_1 is larger than the depth of x with respect to P_2. More precisely, assuming that random samples $X_{11}, \dots, X_{1n_1}$ and $X_{21}, \dots, X_{2n_2}$ from P_1 and P_2, respectively, are available, and denoting as $P_{\ell n}$, $\ell = 1, 2$ the corresponding empirical probability measures, x is classified into P_1 if $D(x, P_{1n}) > D(x, P_{2n})$ and into P_2 if $D(x, P_{1n}) < D(x, P_{2n})$ (classification is performed randomly if both depths are equal). A common issue in the field results from the vanishing property of many depths: in the Euclidean case, supervised classification based on, for example, the Tukey (1975) half-space depth or the Liu (1990) simplicial depth, will always classify randomly an observed location x that would be outside the convex hull of both samples; we refer to Francisci, Nieto-Reyes and Agostinelli (2020) for an interesting discussion. Since the same problem may materialize on the sphere, the nonvanishing nature of our spherical depth is an asset for supervised classification and makes it an appealing alternative to the *angular half-space depth* from Liu and Singh (1992) that suffers from this vanishing property.

[4]If one forgets the Jacobian matrix π_m^{-1}, then this second term provides exactly the asymptotics in the Euclidean case for the pushed forward probability measure $\pi_m \# P_{-m}$ for a fixed m.

To compare the performances of max-depth classifiers associated with various depths, we conducted the following Monte Carlo exercise. For each dimension $d \in \{3, 6, 12, 18\}$, we generated a training sample of $n = 400$ mutually independent observations, $n_1 = 200$ randomly sampled from P_1 and $n_2 = 200$ randomly sampled from P_2, for two probability measures P_1, P_2 on $\mathcal{S}^{d-1}$. In each case, we further generated a test sample of $\ell = 400$ mutually independent observations, again $\ell_1 = 200$ from P_1 and $\ell_2 = 200$ from P_2. Each observation from the test sample was then classified into P_1 or P_2 according to four max-depth classifiers using the training sample, namely the max-depth classifiers based on the Mahalanobis depth from Ley, Sabbah and Verdebout (2014), on our hyperspherical spatial depth, on the arc length depth from Liu and Singh (1992) and Pandolfo, Paindaveine and Porzio (2018), and on the angular half-space depth from Liu and Singh (1992). We then recorded the misclassification error rate of each classifier, that is, the proportion of observations from the test sample that were wrongly classified. This was repeated 2500 times, and Figure 4 then provides the resulting boxplots of misclassification error rates for the following pairs (P_1, P_2):

(i) *von Mises–Fisher*: P_1 is the distribution of a random vector X that is von Mises–Fisher with location $m_1 = (0, \dots, 0, 1)' \in \mathbb{R}^d$ and concentration $\kappa = d$, whereas P_2 is the distribution of OX, where O is a rotation matrix fixing the first $d - 2$ canonical basis vectors of $\mathbb{R}^d$ and mapping m_1 to $m_2 = (0, \dots, 0, \sin(\pi/9), \cos(\pi/9))$;

(ii) *Tangent von Mises–Fisher*: for the same m_1 and κ as in (i), the distribution P_1 is the one of

$$X = Zm_1 + \sqrt{1 - Z^2}\begin{pmatrix} S \\ 0 \end{pmatrix},$$

where Z admits the density $z \mapsto c_{d,\kappa}(1 - z^2)^{(d-3)/2} \exp(\kappa z)\mathbb{I}[-1 \le z \le 1]$ ($c_{d,\kappa}$ is a normalizing constant), S follows a von Mises–Fisher distribution with location $(1, 0, \dots, 0)' \in \mathbb{R}^{d-1}$ and concentration $\eta = 5$, and Z and S are mutually independent; P_2 is still the distribution of OX, with the same matrix O as in (i);

(iii) *Tangent elliptical*: the distributions P_1, P_2 are the same as in (ii), but for the fact that S rather results from projecting radially onto $\mathcal{S}^{d-2}$ a $(d - 1)$-variate normal random vector with mean zero and covariance matrix $\Sigma = \operatorname{diag}(100, 1, \dots, 1)$;

(iv) *Dependence in longitude–latitude*: here, P_1 is the distribution of

$$X = \big(U_1(\sin W), \dots, U_{d-1}(\sin W), \cos W\big)',$$

where $U = (U_1, U_2, \dots, U_{d-1})'$ is uniformly distributed on $\mathcal{S}^{d-2}$, and W, conditional on $[T = t]$, is uniform over $[0, \pi\{t(2\pi - t)/\pi^2\}^{3/2}]$, with T defined as the random variable with values in $[0, 2\pi)$ such that $(U_1, U_2) = \sqrt{U_1^2 + U_2^2}(\cos T, \sin T)$; P_2 is still the distribution of OX, with the same rotation matrix O as in the previous cases.

Inspection of Figure 4 reveals that the classifiers based on our hyperspherical spatial depth perform very well overall. In particular, they outperform their Mahalanobis depth and arc length depth competitors in the setup (iii), and they also strongly dominate the arc length depth classifier in setup (iv). While the proposed classifier also slightly dominates the angular half-space depth in the setups (i), (ii), and (iv), the opposite happens in the setup (iii); a crucial drawback of angular half-space depth, however, is that computational issues strictly restrict its use to dimension $d = 3$ (even in dimension 3, computation in the present simulation was only made possible by a recent implementation kindly provided to us by Professor Stanislav Nagy, based on Dyckerhoff and Nagy (2023)).

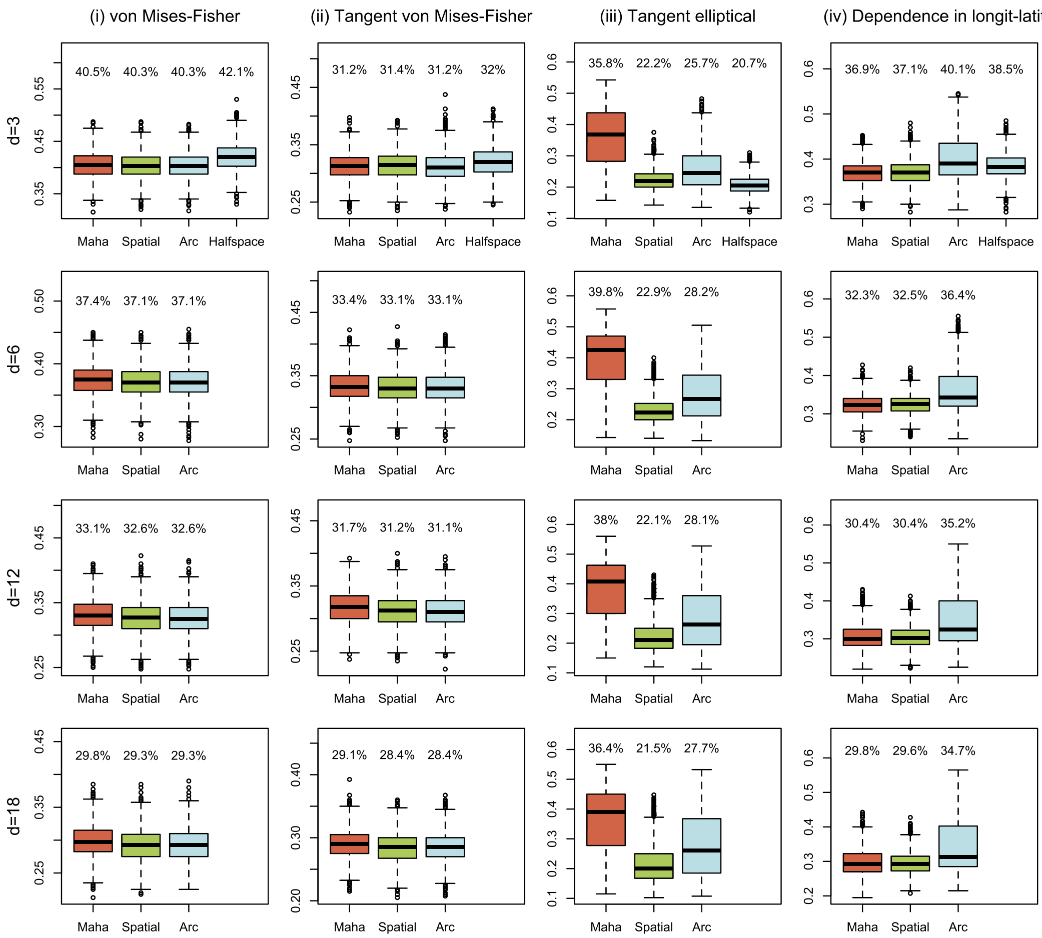

FIG. 4. *Boxplots of misclassification error rates for the max-depth classifiers based on the Mahalanobis depth, our spatial depth, the arc length depth, and the angular half-space depth; results are based on* 2500 *replications, and on balanced training and test samples of size* 400. *We refer to Section* 7.1 *for details on the distributional setups* (*i*)–(*iv*).

7.2. *Testing for rotational symmetry.* As a second application, we consider the problem of testing the null hypothesis that a probability measure $P \in \mathcal{P}_{d-1}$ is rotationally symmetric with respect to the specified median location m (for the sake of simplicity, we assume throughout that P admits a density with respect to the surface area measure on $\mathcal{S}^{d-1}$). It follows from Theorem 5.1 that, under the null hypothesis, $Q_P^m(\alpha u) = (\cos\varphi_\alpha)m + (\sin\varphi_\alpha)u =: z^m_{\varphi_\alpha,u}$ for some $\varphi_\alpha \in [0,\pi]$. Since, under the assumptions adopted here, R_P^m and Q_P^m are inverse maps of one another, and this implies that

$$R_P^m(z^m_{\varphi,u}) = \lambda_\varphi u \quad \text{with } \lambda_\varphi := \int_{\mathcal{U}_m} \| R_P^m(z^m_{\varphi,u})\| \, d\sigma_m(u),$$

where $\mathcal{U}_m$ denotes the collection of unit vectors in $T_m\mathcal{S}^{d-1}$ and σ_m is the surface area measure on $\mathcal{U}_m$, it is then expected that

$$T_P^m := \int_0^\pi \int_{\mathcal{U}_m} \left\| R_P^m(z^m_{\varphi,u}) - \left(\int_{\mathcal{U}_m} \| R_P(z^m_{\varphi,v})\| \, d\sigma_m(v)\right) u \right\|^2 d\sigma_m(u)\, d\varphi$$

measures deviations from rotational symmetry about m. We have the following result.

THEOREM 7.1. *Let $P \in \mathcal{P}_{d-1}$ admit a density on $\mathcal{S}^{d-1}$. Then $T_P^m = 0$ if and only if P is rotationally symmetric with respect to m.*

Assume now that a random sample $X_1, \dots, X_n$ from P is available and denote the corresponding empirical measure by P_n. Theorem 7.1 suggests that the test rejecting the null hypothesis of rotational symmetry about m for large values of

$$T^m_{P_n} := \int_0^\pi \int_{\mathcal{U}_m} \left\| R^m_{P_n}(z^m_{\varphi,u}) - \left(\int_{\mathcal{U}_m} \|R_{P_n}(z^m_{\varphi,v})\|\, d\sigma_m(v)\right) u \right\|^2 d\sigma_m(u)\, d\varphi \tag{7.1}$$

is an omnibus test (i.e., is consistent against any alternative). Deriving the asymptotic null distribution of this test statistic would obviously require a stochastic process version of the asymptotic result in Theorem 6.2(ii). Not only is such a result beyond the scope of the present work, but it would also provide an asymptotic distribution that depends on the particular null distribution P at hand. Here, we favor a more efficient approach relying on exact distribution-freeness. Let $R_n = (R_{n1}, \dots, R_{nn})$ and $U_n = (U_{n1}, \dots, U_{nn})$, where R_{ni} is the rank of $X_i'm$ among $X_1'm, \dots, X_n'm$ and $U_{ni} := (I_d - mm')X_i/\|(I_d - mm')X_i\|$, $i = 1, \dots, n$. Under the null hypothesis of rotational symmetry about m, R_n is uniformly distributed over all permutations of $\{1, \dots, n\}$, the U_{ni}'s form a random sample from the uniform distribution over $\mathcal{U}_m$, and R_n and U_n are mutually independent. As a corollary, denoting as $\tilde{P}_n$ the empirical probability measure associated with the transformed sample

$$\tilde{X}_i = \frac{R_{ni}}{n+1} m + \sqrt{1 - \left(\frac{R_{ni}}{n+1}\right)^2}\, U_{ni}, \quad i = 1, \dots, n,$$

the test statistic $T^m_{\tilde{P}_n}$ is distribution-free under the null hypothesis (note that the $\tilde{X}_i$'s form a random sample from a distribution that is rotationally symmetric about m if and only if the X_i's do). Thanks to distribution-freeness, critical values can of course be arbitrarily well approximated through simulations; more precisely, at level $\alpha \in (0, 1)$, the corresponding test will reject the null hypothesis if and only if

$$T^m_{\tilde{P}_n} > c_\alpha(G), \tag{7.2}$$

where $c_\alpha(G)$ is the sample $(1-\alpha)$-quantile in a collection of G mutually independent values of $T^m_{\tilde{P}_n}$ under the null hypothesis (from distribution-freeness, these G values can be obtained by simulating from an arbitrary distribution that is rotationally symmetric about m).

We explored the finite-sample performances of this test in dimensions $d = 3$ and $d = 4$ through the following Monte Carlo exercise. We generated $M = 2500$ independent random samples of size $n = 200$ for the null hypothesis and some alternatives associated with three different distributions on $\mathcal{S}^{d-1}$. The three distributions are as follows (in each case, $\ell = 0$ will correspond to the null hypothesis of rotational symmetry about $m = (0, \dots, 0, 1)' \in \mathbb{R}^d$, whereas $\ell = 1, 2, 3, 4$ will provide increasingly severe alternatives):

(i) *Tangent von Mises–Fisher*: for $\kappa = 1$, the first distribution is the one of

$$Zm + \sqrt{1 - Z^2} \begin{pmatrix} S \\ 0 \end{pmatrix},$$

where Z admits the density $z \mapsto c_{d,\kappa}(1 - z^2)^{(d-3)/2} \exp(\kappa z) \mathbb{I}[-1 \le z \le 1]$ ($c_{d,\kappa}$ is a normalizing constant), S follows a von Mises–Fisher distribution with location $(1, 0, \dots, 0)' \in \mathbb{R}^{d-1}$ and concentration $\eta_\ell = \ell d/30$, and Z and S are mutually independent;

(ii) *Tangent elliptical*: this distribution is the same as in (i), but for the fact that S rather results from projecting radially onto $\mathcal{S}^{d-2}$ a $(d-1)$-variate normal random vector with mean zero and covariance matrix $\Sigma_\ell = \mathrm{diag}((1 + \ell d^2/20)^2, 1, \dots, 1)$;

(iii) *Dependence in longitude–latitude*: this last distribution is the one of

$$\big(U_1(\sin W), \dots, U_{d-1}(\sin W), \cos W\big)',$$

where $U = (U_1, U_2, \dots, U_{d-1})'$ is uniformly distributed on S^{d-2}, and W, conditional on $[T = t]$, is uniform over $[0, \pi\{t(2\pi - t)/\pi^2\}^{\ell d/6}]$, with T defined as the random variable with value in $[0, 2\pi)$ such that $(U_1, U_2) = \sqrt{U_1^2 + U_2^2}(\cos T, \sin T)$.

In each sample, we performed the following five tests at nominal level $\alpha = 5\%$: (1) the proposed distribution-free spatial test above, where the critical value was obtained from $G = 50{,}000$ independent random samples generated from the von Mises–Fisher distribution with location $m = (0, \dots, 0, 1)' \in \mathbb{R}^d$ and concentration $\kappa = 1$ (both to obtain its critical value then to perform the test, evaluation of the integrals in (7.1) was done along regular grids of size 30 for both φ and u in dimension 3, and along regular grids of size 30 for φ and of size 30×15 for u—30 values for the longitude of u and 15 values for its latitude—in dimension 4); (2) the semiparametric (LV) test from Ley and Verdebout (2017b); (3)–(4) The "location" and "scatter" tests from García-Portugués, Paindaveine and Verdebout (2020), that are optimal against tangent von Mises–Fisher alternatives and tangent elliptical alternatives, respectively; (5) the test of rotational symmetry based on Kuiper's celebrated test of uniformity over $\mathcal{S}^{d-2} = \mathcal{S}^1$, so that this test of rotational symmetry can be used in dimension $d = 3$ only; see page 99 in Mardia and Jupp (2000).

The resulting rejection frequencies are plotted against ℓ in Figure 5. In line with distribution-freeness, the proposed test shows the target size under the null hypothesis in all setups (i)–(iii). Clearly, the test exhibits power against the three types of alternatives considered (which was expected in view of Theorem 7.1), but these simulations reveal that it is the only test that does so among the five tests considered here: the scatter test is blind to alternatives in setup (i), the LV test and location test are blind to alternatives in setup (ii) (both for $d = 3$ and $d = 4$, the blue curve is mostly hidden behind the orange curve), and the Kuiper test is blind to alternatives in setup (iii). The proposed test performs in particular very well against alternatives in setup (i) since it competes almost equally with the optimal location test for such alternatives.

We conclude this section by quickly applying the various tests to the real data set from astronomy considered in García-Portugués, Paindaveine and Verdebout (2020). The data set contains observations of sunspots locations. Sunspots are darker regions on the photosphere of the sun that correspond to solar magnetic field concentrations. Since visual inspection of the data on $\mathcal{S}^2$ may suggest that rotational symmetry holds with respect to $m = (0, 0, 1)$, it is of interest, in order to model sunspots locations, to investigate whether these are compatible with a rotationally symmetric distribution. For the 23rd solar cycle (August 1996–December 2008), which contains $n = 5373$ sunspot locations, the p-values of the spatial test,[5] LV test, location test, scatter test, and Kuiper test are 0.184, 0.431, 0.457, 0.166 and 0.366, respectively, so that, at the usual significance levels, none of the tests rejects the null hypothesis of rotational symmetry about m. For the 22nd cycle (September 1986–July 1996), which includes $n = 4551$ sunspots locations, the corresponding p-values are rather 0.039, 0.012, 0.013, 0.108 and 0.007, respectively, so that all tests, except the scatter test, reject the null hypothesis at level 5%. While one should of course refrain from drawing conclusions based on two data sets only, the p-values of the proposed test that are smaller than the most conservative test in each case, are compatible with its omnibus nature.

[5]Just like the critical value of our test at level α is the $(1-\alpha)$-quantile in a collection of G mutually independent values of the test statistic obtained under the null hypothesis, the corresponding p-value can be evaluated as the proportion of these G values exceeding the value taken by the test statistic on the sample at hand.

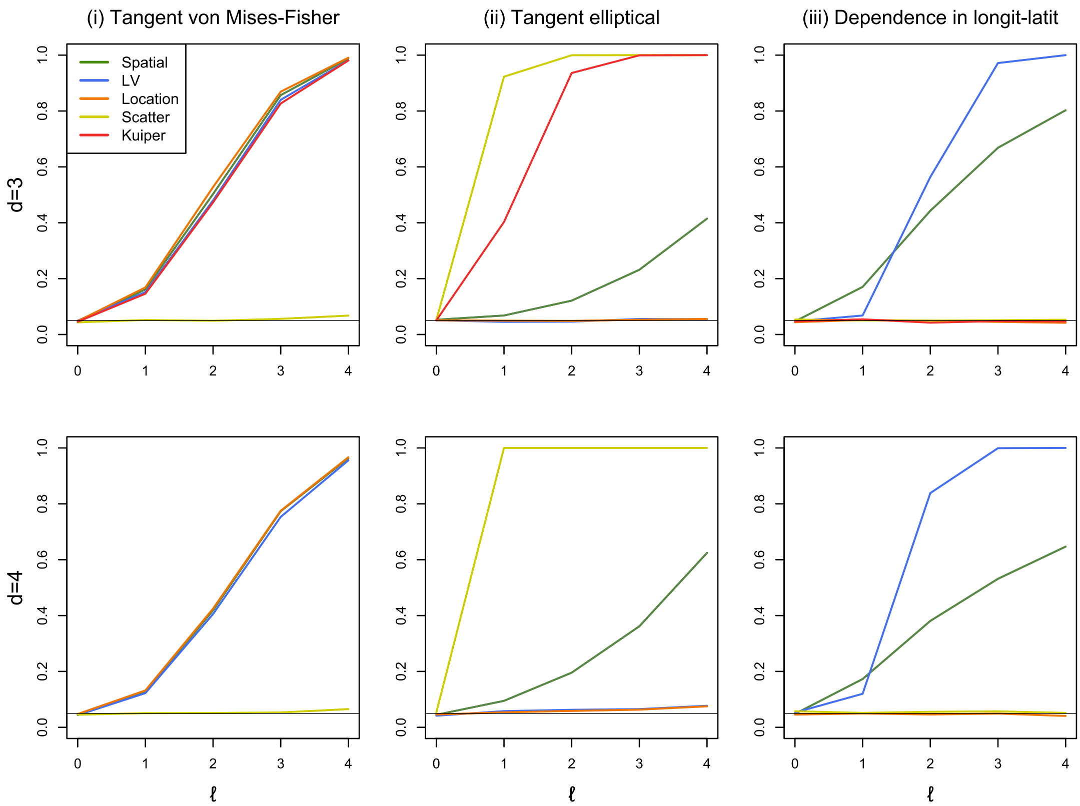

FIG. 5. *Rejection frequencies of five tests of rotational symmetry about $m = (0, \dots, 0, 1)' \in \mathbb{R}^d$ (each test is performed at nominal level $\alpha = 5\%$) based on $M = 2500$ mutually independent random samples of size $n = 200$ drawn from three different models (i)–(iii); in each case, $\ell = 0$ corresponds to the null hypothesis and $\ell = 1, 2, 3, 4$ provide increasingly severe alternatives. We refer to Section 7.2 for details on the five tests and the three models used here.*

8. Final comments. The present work introduced a concept of spatial quantiles for probability measures on unit spheres in arbitrary dimension d. We showed in the paper that the proposed objects inherit many of the nice properties of their Euclidean spatial antecedents. In particular, spherical spatial quantiles characterize the underlying distribution, and they are equivariant under orthogonal transformations (recall that affine transformations are not properly defined on spheres). Just as their Euclidean antecedents, the proposed spherical quantiles also naturally provide companion concepts of ranks and depth. Like in $\mathbb{R}^d$, the resulting depth does not suffer from the vanishing property, which makes it a natural candidate to perform supervised classification on spheres. As we showed, the sample version of our spherical quantiles also allow for explicit asymptotic results. We now close this paper by commenting on further nice properties that are inherited from Euclidean spatial quantiles.

As mentioned at the end of Section 2, Euclidean spatial quantiles can be computed efficiently in virtually any dimension d. Clearly, this extends to the proposed spherical quantiles. Computation of these spherical quantiles indeed only requires three ingredients: (1) performing the direct (resp., inverse) stereographic projections, which is trivial since these are available in closed forms; see (2.2) (resp., (S.6.3)). (2) Computing the sample Fréchet median of n data points in $\mathcal{S}^{d-1}$, which can be achieved very efficiently through the function `frechetMedian` in the recent `R` package *manifold*; see Dai and Lin (2022). (3) Evaluating Euclidean spatial quantiles, which as just recalled, does not raise any challenge even in high dimensions (since such quantiles are minimizers of a simple convex objective function). This explains why spherical spatial quantiles can be easily computed in high dimensions, too. We stress that, on the contrary, even the most recent methods to compute angular half-space depth are limited to $d = 3$ and happen to be extremely slow compared to those providing spatial quantiles, and even more so compared to those evaluating spherical spatial depth, since the latter depth is available in closed form.

Finally, we point out that the proposed spherical quantiles also inherit the good robustness properties of their Euclidean antecedents (it is easy to show that Euclidean spatial quantiles of order α have a breakdown point of at least $(1-\alpha)/2$). Robustness of Euclidean spatial quantiles is actually an important asset in our construction, since, as pointed out by an anonymous referee, the stereographic projection will send possible data points in a small neighborhood of $-\hat{m}_n$ far from the origin of $T_{\hat{m}_n}\mathcal{S}^{d-1}$ and in possibly very different directions. For low to intermediate orders α, the good robustness properties of Euclidean spatial quantiles will ensure that this does not affect too severely the corresponding spherical quantiles. For extreme quantile orders (α large), the robustness of Euclidean spatial quantiles is poorer, but these quantiles will anyway be far from the origin of $T_{\hat{m}_n}\mathcal{S}^{d-1}$, so that the inverse stereographic projection will map these Euclidean quantiles back close to $-\hat{m}_n$ (as it should be), irrespective of the directions in which these quantiles are to be found in the tangent space. In this sense, the natural robustness properties of Euclidean spatial quantiles controls the instability that might have resulted from using the stereographic projection.

Acknowledgments. The author would like to thank the Editor, Professor Lan Wang, the Associate Editor, and two anonymous referees for their insightful comments and suggestions, that led to an important improvement of the paper. They are also grateful to Professor Stanislav Nagy for providing the R code that allowed them to include classifiers based on angular half-space depth in Section 7.1.

Funding. The first author is supported by an Aspirant fellowship from the FNRS (Fonds National pour la Recherche Scientifique), Communauté Française de Belgique. The second author is supported by the Program of Concerted Research Actions (ARC) of the Université libre de Bruxelles and by a grant from the Fonds Thelam, King Baudouin Foundation.

SUPPLEMENTARY MATERIAL

Supplement (DOI: 10.1214/23-AOS2332SUPP; .pdf). The supplement provides the proof of all theorems stated in this paper.

REFERENCES

AGOSTINELLI, C. and ROMANAZZI, M. (2013). Nonparametric analysis of directional data based on data depth. *Environ. Ecol. Stat.* **20** 253–270. MR3068658 https://doi.org/10.1007/s10651-012-0218-z

BHATTACHARYA, R. and LIN, L. (2017). Omnibus CLTs for Fréchet means and nonparametric inference on non-Euclidean spaces. *Proc. Amer. Math. Soc.* **145** 413–428. MR3565392 https://doi.org/10.1090/proc/13216

BHATTACHARYA, R. and PATRANGENARU, V. (2003). Large sample theory of intrinsic and extrinsic sample means on manifolds. I. *Ann. Statist.* **31** 1–29. MR1962498 https://doi.org/10.1214/aos/1046294456

BROWN, B. M. (1983). Statistical uses of the spatial median. *J. Roy. Statist. Soc. Ser. B* **45** 25–30. MR0701072

CARDOT, H., CÉNAC, P. and GODICHON-BAGGIONI, A. (2017). Online estimation of the geometric median in Hilbert spaces: Nonasymptotic confidence balls. *Ann. Statist.* **45** 591–614. MR3650394 https://doi.org/10.1214/16-AOS1460

CARDOT, H., CÉNAC, P. and ZITT, P.-A. (2013). Efficient and fast estimation of the geometric median in Hilbert spaces with an averaged stochastic gradient algorithm. *Bernoulli* **19** 18–43. MR3019484 https://doi.org/10.3150/11-BEJ390

CHAKRABORTY, A. and CHAUDHURI, P. (2014). The spatial distribution in infinite dimensional spaces and related quantiles and depths. *Ann. Statist.* **42** 1203–1231. MR3224286 https://doi.org/10.1214/14-AOS1226

CHAUDHURI, P. (1996). On a geometric notion of quantiles for multivariate data. *J. Amer. Statist. Assoc.* **91** 862–872. MR1395753 https://doi.org/10.2307/2291681

CHENG, Y. and DE GOOIJER, J. G. (2007). On the uth geometric conditional quantile. *J. Statist. Plann. Inference* **137** 1914–1930. MR2323873 https://doi.org/10.1016/j.jspi.2006.02.014

CHERNOZHUKOV, V., GALICHON, A., HALLIN, M. and HENRY, M. (2017). Monge-Kantorovich depth, quantiles, ranks and signs. *Ann. Statist.* **45** 223–256. MR3611491 https://doi.org/10.1214/16-AOS1450

CHOWDHURY, J. and CHAUDHURI, P. (2019). Nonparametric depth and quantile regression for functional data. *Bernoulli* **25** 395–423. MR3892324 https://doi.org/10.3150/17-bej991

DAI, X. and LIN, Z. (2022). manifold: Operations for Riemannian Manifolds. R package version 0.1.1.

DAI, X. and LOPEZ-PINTADO, S. (2023). Tukey's depth for object data. *J. Amer. Statist. Assoc.* **118** 1760–1772. MR4646604 https://doi.org/10.1080/01621459.2021.2011298

DAI, X. and MÜLLER, H.-G. (2018). Principal component analysis for functional data on Riemannian manifolds and spheres. *Ann. Statist.* **46** 3334–3361. MR3852654 https://doi.org/10.1214/17-AOS1660

DYCKERHOFF, R. and NAGY, S. (2023). Exact computation of angular halfspace depth. *Manuscript in Preparation*.

ELTZNER, B. and HUCKEMANN, S. F. (2019). A smeary central limit theorem for manifolds with application to high-dimensional spheres. *Ann. Statist.* **47** 3360–3381. MR4025745 https://doi.org/10.1214/18-AOS1781

FRANCISCI, G., NIETO-REYES, A. and AGOSTINELLI, C. (2020). Generalization of the simplicial depth: No vanishment outside the convex hull of the distribution support. Available at arXiv:1909.02739v2.

FRÉCHET, M. (1948). Les éléments aléatoires de nature quelconque dans un espace distancié. *Ann. Inst. Henri Poincaré* **10** 215–310. MR0027464

GARCÍA-PORTUGUÉS, E., PAINDAVEINE, D. and VERDEBOUT, T. (2020). On optimal tests for rotational symmetry against new classes of hyperspherical distributions. *J. Amer. Statist. Assoc.* **115** 1873–1887. MR4189764 https://doi.org/10.1080/01621459.2019.1665527

GHOSH, A. K. and CHAUDHURI, P. (2005). On maximum depth and related classifiers. *Scand. J. Stat.* **32** 327–350. MR2188677 https://doi.org/10.1111/j.1467-9469.2005.00423.x

GIRARD, S. and STUPFLER, G. (2015). Extreme geometric quantiles in a multivariate regular variation framework. *Extremes* **18** 629–663. MR3418771 https://doi.org/10.1007/s10687-015-0226-0

GIRARD, S. and STUPFLER, G. (2017). Intriguing properties of extreme geometric quantiles. *REVSTAT* **15** 107–139. MR3614901 https://doi.org/10.4310/jsg.2017.v15.n1.a4

HALLIN, M., DEL BARRIO, E., CUESTA-ALBERTOS, J. and MATRÁN, C. (2021). Distribution and quantile functions, ranks and signs in dimension d: A measure transportation approach. *Ann. Statist.* **49** 1139–1165. MR4255122 https://doi.org/10.1214/20-aos1996

HALLIN, M., PAINDAVEINE, D. and ŠIMAN, M. (2010). Multivariate quantiles and multiple-output regression quantiles: From L_1 optimization to halfspace depth. *Ann. Statist.* **38** 635–669. MR2604670 https://doi.org/10.1214/09-AOS723

JUPP, P. E. and KUME, A. (2020). Measures of goodness of fit obtained by almost-canonical transformations on Riemannian manifolds. *J. Multivariate Anal.* **176** 104579. MR4045270 https://doi.org/10.1016/j.jmva.2019.104579

KENDALL, W. S. and LE, H. (2011). Limit theorems for empirical Fréchet means of independent and non-identically distributed manifold-valued random variables. *Braz. J. Probab. Stat.* **25** 323–352. MR2832889 https://doi.org/10.1214/11-BJPS141

KOLTCHINSKII, V. I. (1997). M-estimation, convexity and quantiles. *Ann. Statist.* **25** 435–477. MR1439309 https://doi.org/10.1214/aos/1031833659

KONEN, D. and PAINDAVEINE, D. (2023). Supplement to "Spatial quantiles on the hypersphere." https://doi.org/10.1214/23-AOS2332SUPP

LEY, C., SABBAH, C. and VERDEBOUT, T. (2014). A new concept of quantiles for directional data and the angular Mahalanobis depth. *Electron. J. Stat.* **8** 795–816. MR3217789 https://doi.org/10.1214/14-EJS904

LEY, C. and VERDEBOUT, T. (2017a). *Modern Directional Statistics*. *Chapman & Hall/CRC Interdisciplinary Statistics Series*. CRC Press, Boca Raton, FL. MR3752655

LEY, C. and VERDEBOUT, T. (2017b). Skew-rotationally-symmetric distributions and related efficient inferential procedures. *J. Multivariate Anal.* **159** 67–81. MR3668548 https://doi.org/10.1016/j.jmva.2017.02.010

LI, J., CUESTA-ALBERTOS, J. A. and LIU, R. Y. (2012). DD-classifier: Nonparametric classification procedure based on DD-plot. *J. Amer. Statist. Assoc.* **107** 737–753. MR2980081 https://doi.org/10.1080/01621459.2012.688462

LIU, R. Y. (1990). On a notion of data depth based on random simplices. *Ann. Statist.* **18** 405–414. MR1041400 https://doi.org/10.1214/aos/1176347507

LIU, R. Y. and SINGH, K. (1992). Ordering directional data: Concepts of data depth on circles and spheres. *Ann. Statist.* **20** 1468–1484. MR1186260 https://doi.org/10.1214/aos/1176348779

MARDIA, K. V. and JUPP, P. E. (2000). *Directional Statistics*. *Wiley Series in Probability and Statistics*. Wiley, Chichester. MR1828667

McKeague, I. W., López-Pintado, S., Hallin, M. and Šiman, M. (2011). Analyzing growth trajectories. *J. Dev. Orig. Health Dis.* **2** 322–329.

Nagy, S. (2021). Halfspace depth does not characterize probability distributions. *Statist. Papers* **62** 1135–1139. MR4262188 https://doi.org/10.1007/s00362-019-01130-x

Paindaveine, D. and Virta, J. (2021). On the behavior of extreme d-dimensional spatial quantiles under minimal assumptions. In *Advances in Contemporary Statistics and Econometrics—Festschrift in Honor of Christine Thomas-Agnan* (A. Daouia and A. Ruiz-Gazen, eds.) 243–259. Springer, Cham. MR4299283 https://doi.org/10.1007/978-3-030-73249-3_13

Pandolfo, G., Paindaveine, D. and Porzio, G. C. (2018). Distance-based depths for directional data. *Canad. J. Statist.* **46** 593–609. MR3902616 https://doi.org/10.1002/cjs.11479

Serfling, R. J. (2002). Quantile functions for multivariate analysis: Approaches and applications. *Stat. Neerl.* **56** 214–232.

Tukey, J. W. (1975). Mathematics and the picturing of data. In *Proceedings of the International Congress of Mathematicians* (*Vancouver*, *B.C.*, 1974), *Vol.* 2 523–531. Canad. Math. Congr., Montreal, QC. MR0426989

Tyler, D. E. (1987). Statistical analysis for the angular central Gaussian distribution on the sphere. *Biometrika* **74** 579–589. MR0909362 https://doi.org/10.1093/biomet/74.3.579

Wang, X., Zhu, J., Pan, W., Zhu, J. and Zhang, H. (2021). Nonparametric statistical inference via metric distribution function in metric spaces. Available at arXiv:2107.07317.

Wei, Y. (2008). An approach to multivariate covariate-dependent quantile contours with application to bivariate conditional growth charts. *J. Amer. Statist. Assoc.* **103** 397–409. MR2420242 https://doi.org/10.1198/016214507000001472

Yang, L. (2011). Some properties of Fréchet medians in Riemannian manifolds. ArXiv preprint. Available at arXiv:1110.3899v2.

Zuo, Y. and Serfling, R. (2000). General notions of statistical depth function. *Ann. Statist.* **28** 461–482. MR1790005 https://doi.org/10.1214/aos/1016218226